▪ Journal of Competitiveness

Spatiotemporal Forecasting of Urban Financial Risk in the Yangtze River Delta

Weiran Lin, Haijing Yu, Caihong Zhu*

Abstract

Urban financial stability is essential for sustainable regional development and the resilience of urban economic systems. However, existing studies provide limited city-level measurement of urban financial risk and rarely account for spatial interactions among cities. This study addresses these gaps by developing an integrated framework for the measurement and forecasting of urban financial risk in the Yangtze River Delta. A multidimensional indicator system is constructed, covering macroeconomic conditions, banking system risk, real estate market risk, and government finance and debt risk, with environmental factors and implicit local government debt risk indicators incorporated to capture emerging sources of financial vulnerability. Using panel data for 27 cities from 2008 to 2023, a dynamic composite evaluation method with an acceleration effect is applied to measure urban financial risk and analyze its spatiotemporal evolution, revealing significant spatial heterogeneity and clustering across cities. To further enhance predictive performance, a spatiotemporal forecasting framework is developed by integrating Graph Convolutional Networks (GCNs) with temporal deep learning models, where a trainable adjacency matrix is employed to capture inter-urban dependence. Empirical results show that the proposed models outperform benchmark time-series models, with the Serial Long Short-Term Memory–GCN model achieving the best performance in terms of R^2 and RMSE. Overall, the findings demonstrate that incorporating spatial dependence into temporal modeling significantly improves forecasting accuracy, providing methodological contributions to urban financial risk analysis and supporting the development of more effective early-warning systems.

Keywords: *urban financial risk, dynamic composite measurement, spatiotemporal modeling, graph neural networks, Yangtze River Delta*

JEL Classification: G01, R12, C55

Article history: Received: May 2025; Accepted: September 2026; Published: September 2026

1 INTRODUCTION

Amid profound global economic restructuring and rapid financial innovation, financial stability has become a cornerstone of sustainable development. Major shocks, such as the 2008 global financial crisis and the COVID-19 pandemic, have highlighted the cross-sectoral and cross-regional transmission of financial risks, often described as a "domino effect" (Reinhart & Rogoff, 2009; Claessens et al., 2010; Allen et al., 2012; Zhang et al., 2020; Akhtaruzzaman et al., 2021; Moutinho et al., 2025; Qi et al., 2025; Urom et al., 2026). As regional risks accumulate and propagate through spatial linkages, strengthening monitoring and early-warning systems is essential to safeguarding macroeconomic stability (Chen et al., 2020; Zhuang & Wei, 2023; Li et al., 2024; An et al.,2025).

Existing international research on financial risk has primarily focused on systemic risks at the national level or on cross-country contagion in the context of globalization, with particular emphasis on intermarket linkages and spillover effects (Gai & Kapadia, 2010; Guesmi et al.,

https://doi.org/10.7441/joc.2026.03.01

2018; Arbia et al., 2018; Park & Shin, 2020; Gil-Alana et al., 2020; Inekwe, 2021; Le et al., 2022; Giua et al., 2024; Gaigaliene & Jurakovaite, 2024; Hetzer & Burgoon, 2024; Parashar et al., 2026; Kong & Zhang, 2026; Hu et al., 2026). By contrast, in large economies such as China, financial risks display pronounced regional heterogeneity. Existing domestic studies primarily examine regional financial risk at the provincial or national level using macroeconomic indicators (Shen et al., 2019; Xie & Li, 2020; Zhao & Zhang, 2022; Li et al., 2024; Li et al., 2025). However, city-level analysis remains underexplored, despite cities being key carriers and transmission nodes of urban financial risk, particularly in highly integrated regions such as the Yangtze River Delta (YRD).

Within the YRD, cities differ substantially in economic structure, financial systems, and policy environments, leading to heterogeneous risk profiles. For example, while Shanghai serves as a financial center, nearby cities such as Suzhou, Wuxi, and Hangzhou possess distinct industrial structures and differing levels of exposure to financial risk. Simultaneously, strong intercity linkages in production networks, capital flows, and trade intensify spatial dependence in urban financial risk, allowing shocks to propagate across cities. In addition, fiscal pressure and debt accumulation are often more pronounced at the city level, particularly in less-developed cities. These features make city-level analysis essential for accurately identifying and managing urban financial risk.

Despite growing interest, existing studies on urban financial risk in the YRD face two main limitations. First, current measurement frameworks often fail to incorporate emerging risk factors, such as environmental pressures (Hu et al., 2020; Huang et al., 2020; Zhang et al., 2020; Ma et al., 2022; Huang et al.,2024; Chen et al., 2026) and implicit local government debt (Wang & Huang, 2015; Shen & Shi, 2022; Wan et al.,2024; Wang et al., 2025; Guo & Chen, 2025), and typically rely on static or linear weighting schemes, which may overlook dynamic "acceleration effects" (Yi et al., 2016) in risk evolution. Second, although machine learning approaches—particularly neural networks—have improved early-warning performance (Nag & Mitra, 1999; Kim et al., 2004; Chen et al., 2006; Ahn et al., 2011; Huang & Guo, 2020; Ouyang et al., 2021; Dang et al., 2022), most studies treat cities as independent units, neglecting intercity linkages and spatial dependence in urban financial risk. Graph Neural Networks (GNNs), which are well suited for modeling complex network structures (Kipf & Welling, 2017; Ren et al., 2022; Wang et al., 2024; Wei et al., 2025; Wang et al.,2025; An et al.,2025; Zou et al.,2025; Vega et al., 2025; Xiong et al., 2026), offer advantages for capturing such dependencies but remain underutilized in city-level financial risk analysis.

To address these gaps, this study develops an integrated framework for the measurement and forecasting of urban financial risk in the YRD. First, a multidimensional measurement system is constructed, incorporating emerging risk factors and a dynamic weighting scheme with an acceleration effect. Second, a spatiotemporal forecasting framework based on GNNs is developed, where cities are modeled as nodes and interurban financial relationships are represented as weighted connections, enabling the joint modeling of temporal dynamics and spatial dependence. In addition, textual information is incorporated to enrich model features and improve predictive performance. Finally, the study provides a comprehensive analysis of the spatiotemporal evolution and forecasting of urban financial risk, offering empirical evidence for improving early-warning systems.

The remainder of this study is organized as follows. Section 2 reviews the relevant literature. Section 3 presents the measurement framework of urban financial risk. Section 4 introduces the

https://doi.org/10.7441/joc.2026.03.01

spatiotemporal forecasting models. Section 5 presents the empirical results, including spatiotemporal patterns and model performance. Finally, Section 6 concludes the study.

2 LITERATURE REVIEW

Research on financial risk has increasingly incorporated spatial perspectives, spanning multiple levels from global and national systems to regional and city-level analyses. Existing studies at the global and national levels primarily focus on systemic risk and cross-country contagion, emphasizing financial linkages and spillover effects across markets and regions (Bae et al., 2003; Pascha, 2007; Jung, 2009; Galesi & Sgherri, 2009; Guesmi et al., 2018; Arbia et al., 2018; Zhang et al., 2019; Park & Shin, 2020; Gil-Alana et al., 2020; Inekwe, 2021; Le et al., 2022; Hsiao & Morley, 2022; Giua et al., 2024; Gaigaliene & Jurakovaite, 2024; Hetzer & Burgoon, 2024; Parashar et al., 2026; Kong & Zhang, 2026; Hu et al., 2026). For example, Zhou et al. (2012) and Beirne & Fratzscher (2013) investigated financial contagion during the European debt crisis, while Park & Mercado (2014) analyzed the transmission of financial stress across economies.

In China, owing to data availability constraints, most studies focus on the provincial level, examining the measurement, determinants, and spatial evolution of financial risk (Shen et al., 2019; Xie & Li, 2020; Zhao & Zhang, 2022; Li et al., 2024; Li et al., 2025). By contrast, city-level research remains relatively limited, even though cities serve as key carriers and transmission nodes of urban financial risk, particularly in highly integrated regions such as the YRD.

2.1 Measurement of urban financial risk

Urban financial risk lies between micro-level and macro-level risk, involving multiple dimensions and complex interactions. Existing measurement approaches typically construct indicator systems based on financial markets, selecting variables from banking, securities, insurance, and foreign exchange markets (Chen et al., 2020; Li et al., 2024). Some studies adopt broader multidimensional frameworks, incorporating financial institutions, enterprises, governments, and macroeconomic conditions (Tan, 2010; Shen et al., 2019).

More recent research has begun to consider external shocks; however, emerging risk factors remain insufficiently integrated, particularly environmental pressures and implicit local government debt risk. These factors are especially relevant in the YRD, where rapid urbanization and industrial activity generate significant environmental and fiscal pressures (Hu et al., 2020; Huang et al., 2020; Zhang et al., 2020; Ma et al., 2022; Huang et al.,2024; Chen et al., 2026; Wang et al., 2025; Guo & Chen, 2025).

In terms of methodology, traditional studies primarily rely on static weighting methods, such as AHP, Principal Component Analysis (PCA), entropy, and fuzzy evaluation (Zhong et al., 2002; Shen et al., 2019; Li et al., 2024). These approaches fail to capture dynamic changes in indicator importance. Although dynamic weighting methods have been proposed (Ding et al., 2019), they generally overlook nonlinear acceleration effects in risk evolution, limiting their ability to detect turning points in a timely manner.

2.2 Machine learning and early warning of urban financial risk

Machine learning methods have been widely applied to financial risk early warning. Traditional models such as Logit and SVM enhance classification performance (Kumar et al., 2003; Chen

https://doi.org/10.7441/joc.2026.03.01

et al., 2006; Ahn et al., 2011; Huang & Guo, 2020), while neural networks further improve predictive accuracy (Nag & Mitra, 1999; Kim et al., 2004; Zhao et al., 2022). Recently, deep learning approaches—such as Long Short-Term Memory (LSTM) and deep cross networks—have been applied to financial risk forecasting (Ouyang et al., 2021; Yuan, 2022; Dang et al., 2022).

However, most existing models treat cities as independent units, overlooking spatial dependence and risk spillover across urban areas. In reality, urban financial risk is shaped by complex intercity linkages, including trade, investment, and financial networks (Gai & Kapadia, 2010; Feng et al., 2016; Ding et al., 2019; Shen et al., 2019; Chen et al., 2020; Zhang & Teng, 2021; Ouyang & Xiong, 2023; Gaigaliene & Jurakovaite, 2024; Yang et al.,2024; Xu et al., 2025). This limitation is particularly crucial in the YRD, where cities are highly interconnected.

GNNs provide an effective framework for modeling such complex spatial structures. Since the work of Kipf & Welling (2017), various GNN architectures—including Graph Attention Networks and Graph Isomorphism Networks—have been developed. Recent studies have applied GNNs to analyze inter-industry risk spillovers (Ren et al., 2022).

More recent research further integrates graph neural networks with complex network theory and machine learning methods to enhance systemic risk identification and early-warning performance. For example, Ren et al. (2025) employ a gated graph neural network (GGNN) to model inter-industry tail-risk spillover networks and demonstrate its superior performance in financial crisis prediction. Similarly, Yuan et al. (2026) propose a saliency-fused spatio-temporal graph neural network (SFST-GNN) to capture heterogeneous node effects and dynamic risk amplification in financial systems, significantly improving early-warning accuracy. Beyond financial markets, graph-based and network-driven approaches have also been widely used to model dynamic spillovers and regime-switching behaviors in complex systems (An et al., 2025; Wang et al., 2025), as well as to analyze risk propagation and network structures across global stock markets (Zou et al., 2025) and evolving economic networks (Wei et al., 2025). These studies highlight the growing importance of combining GNNs with network dynamics and machine learning techniques for capturing complex spatial dependence and nonlinear interactions in risk systems.

Nevertheless, applications of GNNs to urban financial risk early warning remain limited, particularly at the city level.

2.3 Research gaps

In summary, the existing literature reveals three major limitations. First, current measurement frameworks for urban financial risk inadequately incorporate emerging factors, particularly environmental pressures and implicit local government debt risk. Second, traditional weighting approaches fail to capture dynamic and nonlinear characteristics of risk evolution, particularly acceleration effects. Third, most forecasting models neglect spatial dependence and interurban risk spillover, limiting their ability to reflect the networked nature of urban financial systems. These limitations highlight the need for an integrated framework that combines multidimensional measurement with spatiotemporal modeling of urban financial risk, particularly in highly interconnected regions such as the YRD.

3 URBAN FINANCIAL RISK MEASUREMENT FRAMEWORK

https://doi.org/10.7441/joc.2026.03.01

3.1 Indicator system for urban financial risk

The YRD urban agglomeration, located at the estuary of the Yangtze River, comprises 27 prefecture-level cities across Shanghai Municipality and the provinces of Jiangsu, Zhejiang, and Anhui. As one of the most economically dynamic and highly integrated regions in China, the YRD plays a pivotal role in national economic development. However, strong intercity linkages, heterogeneous economic structures, and varying financial systems make the region vulnerable to spatial dependence and risk spillover. Localized financial risks may therefore propagate across cities and evolve into broader systemic risks.

To address these challenges, this study develops a multidimensional measurement framework for urban financial risk, guided by the principles of scientific rigor, comprehensiveness, and operability. The framework includes four dimensions: (1) macroeconomic risk; (2) banking system risk; (3) real estate market risk; and (4) government fiscal and debt risk.

Based on these dimensions, a system of 12 secondary indicators is constructed (Tab.1), capturing traditional and emerging sources of financial vulnerability.

Compared with existing studies, this framework incorporates several key innovations: (1) Environmental pressure: Annual average $PM_{2.5}$ concentration is introduced to capture ecological constraints and their impact on economic resilience. (2) Implicit local government debt risk: Urban investment bond credit spreads are used as a proxy for market-perceived fiscal risk. (3) Banking risk proxy: Due to data limitations, the nonperforming loan (NPL) ratio of city-headquartered or rural commercial banks is used to approximate city-level banking risk.

These additions enhance the ability of the framework to reflect emerging and structural sources of urban financial risk.

Tab.1 – Indicator system for measuring urban financial risk. Source: own research

Primary dimensions	Secondary indicators	Relationship to urban financial risk
Macroeconomic risk	Per capita GDP	Negative correlation: Higher per capita income levels imply greater financial resilience.
	GDP growth rate	Negative correlation: Rapid economic growth suggests lower financial vulnerability.
	Net population inflow rate	Negative correlation: A sustained net inflow reflects growth potential and investor confidence.
	Annual average $PM_{2.5}$ concentration	Positive correlation: Elevated pollution levels often reflect outdated industrial structures and limited risk absorption capacity.
Banking system risk	Nonperforming loan ratio	Positive correlation: A higher NPL ratio signals deteriorating credit asset quality.
	Loan-to-deposit ratio	Positive correlation: A high loan-to-deposit ratio may reflect rising liquidity risks.
	Credit-to-GDP ratio	Positive correlation: Excessive credit penetration tends to magnify systemic vulnerabilities.
Real estate market risk	Growth rate of commercial housing sales area	Positive correlation: Rapid transaction growth may signal increasing speculative activity.
	Housing price-to-income ratio	Positive correlation: A rising ratio suggests worsening housing affordability and potential asset bubbles.

https://doi.org/10.7441/joc.2026.03.01

Government fiscal and debt risk	Fiscal balance ratio	Positive correlation: A widening fiscal gap implies reduced fiscal resilience.
	Local government debt-to-GDP ratio	Positive correlation: Higher leverage levels may reflect increased risks of fiscal unsustainability.
	Urban investment credit spread	Positive correlation: An expanding spread reflects heightened market concerns over debt repayment capacity.

3.2 Data sources and processing

The data required for measuring urban financial risk comprise panel data covering 27 cities in the YRD urban agglomeration and 12 indicators (Tab.1). Data were primarily collected from the iFinD Economic Database (EDB). When data were unavailable or incomplete, supplementary information was obtained from the Wind EDB. For any remaining missing values, additional data were manually collected and verified using authoritative sources, including the China Statistical Yearbook, provincial and municipal statistical yearbooks, and official government statistical bulletins. This multisource data collection strategy ensures the completeness and reliability of the dataset.

3.2.1 Macroeconomic risk

In the macroeconomic risk dimension, this study adopts four secondary indicators—per capita GDP, GDP growth rate, net population inflow rate, and annual average $PM_{2.5}$ concentration—to comprehensively capture the economic scale, growth potential, demographic dynamics, and environmental pressure of a city.

(1) Per capita GDP, GDP growth rate, and net population inflow rate: Due to challenges in obtaining consistent and unbiased unemployment rate data at the prefecture and city levels, this study adopts nominal GDP growth rate as a proxy for economic vitality and resilience. The net population inflow rate is derived from the annual growth rate of the permanent population, as follows:

$$NPIR_{it} = \frac{PPEY_{it} - PPEY_{it-1}}{PPEY_{it-1}} \quad (1)$$

where $NPIR_{it}$ denotes the net population inflow rate of city i in year t; $PPEY_{it}$ and $PPEY_{it-1}$ represent the permanent population at the end of year t and $t-1$, respectively. For the missing permanent population data in eight Anhui cities (e.g., Wuhu, Ma'anshan, and Tongling) during 2007–2008, data were manually supplemented using local statistical yearbooks and government bulletins to ensure completeness.

(2) Annual average $PM_{2.5}$ concentration: Given the lack of complete official monitoring data prior to 2013, this study adopts the internationally recognized ACAG satellite retrieval model to estimate city-level $PM_{2.5}$ concentrations, following the methodologies of Geng et al. (2015) and van Donkelaar et al. (2021). Data processing includes the following: (a) For 2008–2014, $PM_{2.5}$ levels are estimated using ACAG satellite-derived data; (b) For 2015–2023, monthly $PM_{2.5}$ measurements from iFinD are used, and annual averages are computed as the mean of monthly values; and (c) For cities with missing data in 2013–2014, values are supplemented using ACAG satellite data to maintain temporal consistency and completeness.

3.2.2 Banking system risk

https://doi.org/10.7441/joc.2026.03.01

In China's predominantly bank-based financial system, banks serve as the primary channels for resource allocation, credit creation, and risk transmission. Based on indicator representativeness and data availability, this study selects three metrics—NPL ratio, loan-to-deposit (LDR) ratio, and credit-to-GDP ratio—to assess the stability of urban banking systems and support the identification of regional financial vulnerabilities.

(1) NPL ratio: Given the scarcity of city-level data, this study adopts a proxy approach, using the NPL ratio reported by urban commercial bank headquarters to represent city-level risk. When multiple urban commercial banks exist, preference is given to the bank sharing the name of the city (e.g., Bank of Nanjing). In the absence of an urban commercial bank, data from local rural commercial banks (e.g., Wuhu Rural Commercial Bank) are utilized. From 2008 to 2023, NPL ratios were directly obtained for 18 of the 27 YRD cities. The remaining nine cities with relatively underdeveloped economies (Yancheng, Zhenjiang, and Taizhou in Jiangsu; Zhoushan in Zhejiang; and Ma'anshan, Tongling, Chuzhou, Chizhou, and Xuancheng in Anhui) primarily engage in financial activities through rural commercial banks. Therefore, the NPL ratio of rural commercial banks is used as a proxy for the NPL ratio of cities with underdeveloped economies. In addition, data gaps existed for certain years in 18 cities: Wuxi, Shaoxing, Suzhou, Haian, and Anqing (1–3 years); Changzhou (2008–2011); Yangzhou (2008–2012); and Wuhu (2008–2013). To address these gaps, the following strategies were employed: first, a calibration of rural commercial bank data was conducted. Since rural commercial banks typically exhibit higher NPL ratios than their urban counterparts, this study applies a correction based on national averages, using the following adjustment formula:

$$NPLR_{it} = NPLR_{it}^{rural} \times \frac{\overline{NPLR}_t^{urban}}{\overline{NPLR}_t^{rural}} \tag{2}$$

where $NPLR_{it}$ is the adjusted nonperforming loan ratio of city i in year t; $NPLR_{it}^{rural}$ is the local rural commercial bank nonperforming loan ratio of city i in year t; $\overline{NPLR}_t^{urban}$ is the national average urban commercial bank nonperforming loan ratio of city i in year t; and $\overline{NPLR}_t^{rural}$ is the national average rural commercial bank nonperforming loan ratio of city i in year t. Second, for cities with partial-year gaps (18 cities), sporadic annual data gaps were interpolated using the proportional growth rate method relative to the corresponding provincial average. Finally, for cities with entirely missing data (nine cities), imputation was conducted using the intra-provincial average of cities with available data in the same year, ensuring regional comparability within the same banking environment.

(2) LDR ratio and credit-to-GDP ratio: For cities with missing year-end data, this study extracts December values from iFinD's monthly datasets using keyword searches, then computes the LDR and credit-to-GDP ratio accordingly. The specific indicator formulas are defined as follows:

$$LDR_{it} = \frac{Loans_{it}}{Deposits_{it}} \tag{3}$$

$$CreditGDP_{it} = \frac{Loans_{it} + Deposits_{it}}{GDP_{it}} \tag{4}$$

where LDR_{it} is the loan-to-deposit ratio of city i in year t; Loans_{it} is the year-end loan balance of city i in year t; and $\mathrm{Deposits}_{it}$ is the year-end deposit balance of city i in year t. $CreditGDP_{it}$ is the credit-to-GDP ratio of city i in year t; and GDP_{it} is the GDP of city i in year t. For missing deposit and loan data in certain Anhui cities (e.g., Tongling and Ma'anshan),

https://doi.org/10.7441/joc.2026.03.01

interpolation is conducted using proportional growth relative to the provincial average as follows:

$$MLDR_{it} = LDR_{it-1} \times \frac{\overline{LDR}_{it}^{prov}}{\overline{LDR}_{it-1}^{prov}} \quad (5)$$

where $MLDR_{it}$ is the missing loan-to-deposit ratio of city i in year t; LDR_{it-1} is the loan-to-deposit ratio of city i in year $t-1$; $\overline{LDR}_{it}^{prov}$ is the average loan-to-deposit ratio of other cities in the province where city i is located in year t; and $\overline{LDR}_{it-1}^{prov}$ is the average loan-to-deposit ratio of other cities in the province where city i is located in year $t-1$. This approach assumes that deposit and loan structure trends are similar across cities within the same province, thereby ensuring the integrity and comparability of the panel dataset. The same proportional interpolation approach as in Equation (5) is applied to subsequent missing values, using provincial-level growth benchmarks.

3.2.3 Real estate market risk

Real estate market risk constitutes a critical component of urban financial vulnerability. Due to the unavailability of consistent city-level data on mortgage balances and rent-to-sale ratios, this study employs two widely accessible and representative indicators: the growth rate of commercial housing sales area, which captures market activity and potential speculative bubbles; and the housing price-to-income ratio, which reflects the housing affordability burden and the degree of price–income deviation.

(1) Growth rate of commercial housing sales area: Primarily derived from city-level commercial housing sales area data in the iFinD EDB covering 2008–2022. For 2023, due to data gaps in several cities, the cumulative annual value as of December is supplemented using monthly data from the Wind database. For cities with partial data gaps from 2014 to 2017, missing values are interpolated using the proportional growth rate method relative to the provincial average.

(2) Housing price-to-income ratio: This indicator reflects the affordability of housing for urban residents and is calculated as follows:

$$HPIR_{it} = \frac{Price_{it}}{Income_{it}} \quad (6)$$

where $HPIR_{it}$ is the housing price-to-income ratio for city i in year t; $Price_{it}$ is the average price of commercial residential buildings at the end of December in city i in year t; and $Income_{it}$ is the per capita disposable income of urban residents in city i in year t. Data on per capita disposable income of urban residents are sourced from the iFinD EDB (2008–2023, new version). The missing 2023 value for Zhenjiang is supplemented using the Wind database. Regarding average commercial housing prices, data from 2019 to 2023 are primarily sourced from the "Zhuge Qihang" module in iFinD, while missing values for Yangzhou and Zhoushan are supplemented with historical records from Jiwu.com. For 2008–2018, official data for Shanghai, Hefei, Nanjing, Hangzhou, and Ningbo are obtained from the National Bureau of Statistics; data for Wuxi are calculated from monthly averages released by the local Housing and Urban–Rural Development Bureau. For the remaining cities, data are sourced from Jiwu.com (2015–2018) and back-calculated for 2008–2014 based on the year-on-year growth rate of provincial average housing prices.

https://doi.org/10.7441/joc.2026.03.01

3.2.4 Government fiscal and debt risk

Local governments in China often adopt large-scale investment-driven strategies for infrastructure development and economic transformation. However, this model frequently results in the rapid accumulation of explicit and implicit debt, posing serious risks to fiscal sustainability and urban financial stability. This study selects three key indicators to comprehensively assess local government fiscal and debt risks: the fiscal revenue–expenditure gap ratio, the local government debt-to-GDP ratio, and the urban investment bond credit spread.

(1) Fiscal balance ratio: This indicator reflects the fiscal balance of local governments and is calculated as follows:

$$FBR_{it} = \frac{Expenditure_{it} - Revenue_{it}}{NomGDP_{it}} \tag{7}$$

where FBR_{it} is the fiscal balance ratio for city i in year t; $Expenditure_{it}$ is the general public budget expenditure of city i in year t; $Revenue_{it}$ is the general public budget revenue in year t; and NomGDP_{it} is the nominal GDP of city i in year t. Missing values are observed in Anqing (2008–2014), Yancheng (2008–2011, 2016), Taizhou (2008–2010), Chuzhou (2009–2010), and Ma'anshan (2009). These gaps are addressed using the provincial-level proportional growth rate method.

(2) Local government debt-to-GDP ratio: This indicator measures the fiscal leverage and debt sustainability of local governments. Data processing is conducted in two distinct stages: for the period 2016–2023, minor missing values are interpolated using the proportional growth rate method relative to the provincial average. For the period 2008–2015, due to significant data gaps, a neural network regression model (Multi-Layer Perceptron, MLP) was used for data imputation. The model incorporates 10 relevant macro-financial variables, such as per capita GDP, GDP growth rate, NPL ratio, and LDR, excluding the target indicators (debt-to-GDP ratio and credit spread) listed in Tab.1. All input data are standardized before model training and prediction.

(3) Urban investment bond credit spread: This indicator reflects the yield premium of urban investment bonds over government bonds of similar maturity, thereby serving as a proxy for the implicit debt risk of local governments. The indicator is computed using a balance-weighted average method, as follows:

$$CSp_{it} = \frac{\sum_{j=1}^{n}(R_{jit}^{UIB} - R_{jt}^{Gov})\cdot B_{jit}}{\sum_{j=1}^{n} B_{jit}} \tag{8}$$

where CSp_{it} is the urban investment credit spread in city i at time t; R_{jit}^{UIB} is the yield of the jth urban investment bond at time t; R_{jt}^{Gov} is the yield of a government bond with matching maturity to bond j at time t; B_{jit} is the outstanding balance of the jth urban investment bond at time t; and n is the total number of urban investment bonds observed. As the credit spread is measured on a daily basis, its annual value is obtained by averaging daily spreads over the year. Due to systematic data gaps from 2008 to 2012, the same neural network regression approach is adopted—using 10 fully available macro-financial indicators as inputs—to impute missing values via nonlinear prediction.

3.3 Dynamic composite measurement method

https://doi.org/10.7441/joc.2026.03.01

Existing dynamic weighting approaches for regional financial risk assessment often overlook the "acceleration" in the evolution of risk indicators, thereby limiting the effectiveness of timely risk identification and prevention. To address this gap, it is essential to develop a dynamic weighting scheme that incorporates the "acceleration" of indicator trajectories, taking into account the joint effects of development trends, indicator weights, and temporal weights. Yi et al. (2016) proposed a dynamic evaluation framework that captures the acceleration effect in indicator evolution and formulated the following model:

$$\varphi_i(x_j, \tau_k, \rho_{jk}, \omega_j) = \sum_{k=1}^{N} \tau_k \sum_{j=1}^{m} \omega_j x_{ijk}^{**} \tag{9}$$

where x_{ijk}^{**} is the indicator value after the action of the "development factor." $\tau_k = \lambda_k / \sum_{k=1}^{N} \lambda_k$ and $\lambda_k = exp(-(k - N)^2/2)$, where $k = 1,2,\ldots,N$. In line with the idea of "valuing the present over the past," τ_k is referred to as the time weight at the k-th moment, increasing as time approaches the present and decreasing for earlier periods. The comprehensive evaluation leverages panel data from 2008 to 2023 (16 years), with set $k = 1$ for 2008 and $k = 16$ for 2023, i.e., $N = 16$. m represents the total number of indicators for comprehensive evaluation; according to Tab.1, this study selected 12 indicators, $m = 12$.

3.3.1 Data standardization

To ensure cross-indicator comparability, this study performs global normalization using the full panel dataset from 2008 to 2023. A global standardization method is applied, distinguishing between positively and negatively correlated indicators, to place all variables on a comparable scale, thereby facilitating weighting and dynamic aggregation. Here, x_{ijk} represents the original value of the j-th indicator of the i-th city in the k-th year, and x_{ijk}^{*} is the standardized value.

$$\text{For positive indicators: } x_{ijk}^{*} = \frac{x_{ijk} - min\, x_{ijk}}{max\, x_{ijk} - min\, x_{ijk}} \tag{10}$$

$$\text{For negative indicators: } x_{ijk}^{*} = \frac{max\, x_{ijk} - x_{ijk}}{max\, x_{ijk} - min\, x_{ijk}} \tag{11}$$

3.3.2 Development factor (acceleration effect)

To capture the dynamic evolution of indicators over time, this study follows the approach proposed by Yi et al. (2016) and introduces a development factor, denoted as ρ_{ijk}, to adjust the standardized indicators through weighted transformation. The corresponding formulation is given as follows:

$$x_{ijk}^{**} = \rho_{ijk} x_{ijk}^{*} \tag{12}$$

where x_{ijk}^{*} denotes the standardized value of indicator j for city i in year k, and ρ_{ijk} represents the development factor, capturing the importance change in that indicator over time. The development factor ρ_{ijk} introduces reward–penalty adjustments to standardized values, embedding the "acceleration" component of trend evolution into the evaluation, thereby enhancing the sensitivity of the model to change as follows:

$$\rho_{ijk} = a - \frac{b}{1 + exp(u_{ijk})} \tag{13}$$

https://doi.org/10.7441/joc.2026.03.01

where a and b are undetermined parameters, depending on the evaluator's preference judgment. Following Yi et al. (2016), this study sets $a = 4.316$ and $b = 6.632$. In addition, $u_{ijk} = \begin{cases} 0 & k = 1 \\ \frac{v_{ijk} - v_{ijk-1}}{t_k - t_{k-1}} & k = 2, \ldots, N \end{cases}$ and $v_{ijk} = \begin{cases} 0 & k = 1 \\ \frac{x^*_{ijk} - x^*_{ijk-1}}{t_k - t_{k-1}} & k = 2, \ldots, N \end{cases}$.

3.3.3 Indicator weighting

To derive ω_j, the study employs the "hierarchical differentiation method" proposed by Guo (2002), which determines indicator weights by maximizing the overall differentiation among evaluated entities. **Step 1**: Determine the annual indicator weights $\omega_{1k}, \omega_{2k}, \ldots, \omega_{mk}$ for each year $k = 1,2, \ldots, N$ by maximizing intercity differentiation as follows:

$$\max \varepsilon^2 = \sum_{i=1}^{n} (y_i(t_k) - \bar{y}(t_k))^2 \tag{14}$$

where $y_i(t_k) = \sum_{j=1}^{m} \omega_{jk} x^{**}_{ijk}$, $\bar{y}(t_k) = \frac{1}{n} \sum_{i=1}^{n} \sum_{j=1}^{m} \omega_{jk} x^{**}_{ijk}$, and n are the number of evaluated objects, which is 27 for the YRD urban agglomeration, i.e., $n = 27$. **Step 2:** Construct an optimization model to minimize the total squared deviation. The optimal weights ω_j are obtained by solving the following program:

$$\max \sigma^2 = \sum_{k=1}^{N} \sum_{i=1}^{n} \sum_{j=1}^{m} \left[(\omega_{jk} - \omega_j) x^{**}_{ijk} \right]^2$$

$$\text{s.t.} \begin{cases} \sum_{j=1}^{m} \omega_j = 1 \\ \omega_j \geq 0, j = 1,2, \ldots, m \end{cases} \tag{15}$$

For a more specific and convenient solution method, reference can be made to the weight calculation method based on the eigenvector corresponding to the maximum eigenvalue proposed by Guo (2002).

4 URBAN FINANCIAL RISK FORECASTING FRAMEWORK

4.1 Forecasting target and predictor variables

This study develops an annual forecasting model for the rate of change in urban financial risk, drawing on panel data from 27 cities in the YRD covering the period 2008–2023. The model incorporates monthly and quarterly authoritative economic indicators issued by national, provincial, and municipal statistical agencies, selected to balance data volume, availability, and conceptual relevance. The model is defined as follows:

$$UFRRC_{it} = f(N_t, P_{p(i)t}, C_{it},) \tag{16}$$

where $UFRRC_{it}$ denotes the urban financial risk rate of change in the i-th city at time t. N_t, $P_{p(i)t}$, and C_{it} are vectors of national, provincial, and city predictors, respectively. The function $f(\cdot)$ is estimated using the LSTM–Graph Convolutional Network (GCN) framework detailed in Section 4.2. The specific predictor variables are listed in Tab.2, comprising 31 secondary indicators in total.

https://doi.org/10.7441/joc.2026.03.01

First, regarding the prediction time point, apart from the 12 variables representing the lagged terms of the "urban financial risk measurement indicators," the remaining 19 leading indicators at the national, provincial, and municipal levels employ first-quarter data of the prediction year (*t*) as inputs to Equation (16).

Second, concerning the prediction target, instead of discretizing the financial risk level—which would require arbitrary threshold settings and could introduce instability—this study continuously predicts the rate of change in urban financial risk, thereby enabling a more precise depiction of its dynamic evolution.

Third, the "policy attention index" is measured as the proportion of financial-risk-related terms appearing in the provincial Government Work Reports issued between January and March of the prediction year. The lagged terms of the "urban financial risk measurement indicator" are derived from the annual data of the previous year, whereas the remaining leading indicators are expressed as year-on-year growth rates.

Finally, the comprehensive lexicon used to construct the "policy attention index" includes the following terms: credit, credit risk, loan risk, default, loan, and micro-loan; interest rate, financing, investment and financing, bonds, venture capital, and real estate; liquidity and leverage; fraud and corruption; supervision, financial supervision, market supervision, supervision zone, customs supervision, and safety supervision; financial risk; and financial crisis.

Tab.2 – Feature indicators for the prediction model. Source: own research

Indicator level	Primary indicators	Secondary indicators	Description
National leading macroeconomic indicators	Investment and Real Estate Leading Indicators	National Real Estate Climate Index	(1) Temporal reference: Model inputs use first-quarter data of the prediction year (t). (2) For indicators released monthly: Following Huh (2002) and Hua (2014), the value at the end of the first quarter (end of March) is used to represent the quarterly indicator.
	Production and Trade Leading Indicators	Manufacturing PMI	
		Total Electricity Consumption: Industrial Electricity Consumption	
		Railway Freight Volume	
	Confidence Leading Indicators	Consumer Index: Confidence Index	
	Monetary and Financial Leading Indicators	New RMB Loans: Medium- and Long-Term Loans	
Provincial-level economic indicators	Policy attention index	Proportion of financial risk-related terms in provincial government work reports	(1) Temporal reference: Based on the release of the provincial "Government Work Report" (January–March) in the prediction year, other quarterly indicators uniformly use the first-quarter-end (end of March) data, and monthly indicators use the March-end value to represent the entire quarter. (2) Construction: Based on provincial Government Work Reports from 2008–2023, financial risk-related terms are extracted using word segmentation techniques, and their frequency is divided by the total word count to produce the annual policy attention index.
	Macroeconomic Performance	GDP (quarterly), CPI (monthly), Value Added of Industries above Designated Size (monthly), Total Retail Sales of Consumer Goods (monthly), Total Imports and Exports	
	Fiscal and Financial Stability	General Public Budget Revenue (monthly), General Public Budget Expenditure (monthly)	
	Investment and Real Estate	Fixed Asset Investment (year-on-year), Real Estate Development Investment	
	Social Livelihood and Infrastructure	Per Capita Disposable Income of Urban Residents	
City-level indicators	Environmental Indicators	City quarterly average $PM_{2.5}$ concentration	(1) Temporal reference: The first-quarter average $PM_{2.5}$ and first-quarter GDP indicators for each city are based on the statistical values for that quarter; the lagged terms of the financial risk indicator use the corresponding values from the previous year.
	Macroeconomic Performance	City GDP (quarterly)	
	Historical Impact of Urban Financial Risk	Lagged terms of urban financial risk measurement indicators	

Note 1. For 2008–2014, the first-quarter average $PM_{2.5}$ concentration is calculated using the same approach as in the urban financial risk measurement framework.

https://doi.org/10.7441/joc.2026.03.01

Note 2. Some potentially informative indicators, such as housing prices and insurance premium income, are excluded because consistent quarterly or monthly city-level data are unavailable, particularly before 2014.

4.2 Spatiotemporal forecasting models for urban financial risk

In the selection of temporal modeling modules, this study adopts LSTM networks and Temporal Convolutional Networks (TCNs) as the foundational models for extracting time-dependent features. Existing research has shown that LSTM models have demonstrated stable and reliable predictive performance in regional financial risk forecasting and other economic–financial applications. Therefore, this study focuses on an LSTM-based temporal modeling approach while incorporating TCN as a comparative extension.

For spatial modeling, a static GCN is employed to construct the interurban financial risk association structure. Compared with dynamic or higher-order GNNs, the static GCN structure is simpler, with fewer parameters, making it more suitable for economic and financial research scenarios with limited sample sizes. This approach helps reduce model complexity, mitigate overfitting, and improve training stability.

4.2.1 Temporal and spatial building blocks

(1) Introduction to the LSTM model: The LSTM network, a specialized Recurrent Neural Network (RNN), excels at modeling long-term dependencies and is widely applied in time series forecasting. Each LSTM unit includes a forget gate (f_t), input gate (i_t), and output gate (o_t). The mathematical formulation and computational processes of these gates are defined in Equations (17)–(22) (Lin et al., 2025).

$$i_t = \sigma(W_i x_t + U_i h_{t-1} + b_i) \tag{17}$$

$$f_t = \sigma(W_f x_t + U_f h_{t-1} + b_f) \tag{18}$$

$$o_t = \sigma(W_o x_t + U_o h_{t-1} + b_o) \tag{19}$$

$$\widehat{c_t} = tanh(W_c x_t + U_c h_{t-1} + b_c) \tag{20}$$

$$c_t = f_t * c_{t-1} + i_t * \widehat{c_t} \tag{21}$$

$$h_t = o_t * \tanh(c_t) \tag{22}$$

Here, W represents the weight matrices for each gate, b denotes the bias vectors, and $\sigma(\cdot)$ is the nonlinear activation function. The symbol "*" represents the element-wise Hadamard product.

(2) Introduction to the GCN model: The GCN effectively processes graph-structured data by aggregating information from nodes and their neighbors. The propagation rule, as proposed by Kipf & Welling (2017), is expressed as follows:

$$\text{Propagation rule of GCN: } H^{(l+1)} = \sigma(\hat{A}H^{(l)}W^{(l)}) \tag{23}$$

where $\hat{A} = D^{-\frac{1}{2}}(A + I)D^{-\frac{1}{2}}$, A denotes the adjacency matrix of the graph, I is the identity matrix, D is the degree matrix of $A + I$, $H^{(l)}$ is the node representation matrix at layer l (with $H^{(0)}$ as the initial node feature matrix), $W^{(l)}$ is the weight matrix at layer l, and $\sigma(\cdot)$ is the nonlinear activation function.

https://doi.org/10.7441/joc.2026.03.01

(3) Introduction to the TCN model: TCNs are a method for modeling time series data based on Convolutional Neural Networks. Unlike RNNs, TCNs capture temporal dependencies through convolutional operations, offering advantages such as parallel computing and improved gradient stability. Given an input time series $x_t = \{x_1, x_2, \ldots, x_T\}$, where x_t represents the input feature at time step ttt, the calculation of the causal convolution in TCN is given as follows:

$$y_t = \sum_{k=0}^{K-1} w_k \cdot x_{t-k} + b \quad (24)$$

where w_k represents the convolution kernel parameters, K is the kernel size (i.e., the length of the time window), and x_{t-k} is the value of the input sequence at time step $t-k$, reflecting the weighted aggregation of the past K time steps' information. The bias term is denoted as b.

In practice, TCN typically comprises multiple stacked layers of 1D convolution modules to progressively extract higher-order features from the time series. The output of the l-th layer convolution network is expressed as follows:

$$y_t^{(l)} = \sigma(\mathrm{TCN}_l(y_t^{(l-1)})) \quad (25)$$

where $y_t^{(l-1)}$ is the output from the previous layer, $\mathrm{TCN}_l(\cdot)$ denotes the convolution operation at the l-th layer, and $\sigma(\cdot)$ is the nonlinear activation function.

4.2.2 Spatiotemporal model architectures

In terms of overall framework design, the spatial branch captures the spillover and contagion mechanisms of financial risk across cities using a GCN, while the temporal branch employs LSTM networks or TCNs to model the temporal dynamics of financial risk within individual cities. Based on different combinations of LSTM, TCN, and GCN, this study constructs four spatiotemporal neural network prediction models: the Serial LSTM–GCN model, the Serial GCN–LSTM model, the Parallel LSTM–GCN model, and the Serial TCN–GCN–TCN model. The overall architecture is shown in Fig. 1.

Given the relatively limited sample size in economic and financial modeling, and to further reduce model parameters and enhance generalization ability, PCA is applied at the input stage to perform dimensionality reduction, removing redundant information and highlighting the key features.

The specific model designs are as follows: **(1) Serial LSTM–GCN Model:** This model first uses an LSTM network to extract the temporal dependency features of financial risk for each city. Subsequently, the temporal features are input into the GCN model to aggregate the spatial risk information across cities. Finally, an MLP maps the combined features to the final prediction variables. **(2) Serial GCN–LSTM Model:** In this model, the GCN model is applied to the input data at each lag period to extract the spatial correlation features across cities, and results are reshaped into time-series data blocks consistent with the original input. The LSTM network then models the temporal dynamics of the spatially aggregated features. The final predictions are obtained through an MLP layer. **(3) Parallel LSTM–GCN Model:** In this configuration, the GCN model is applied to the input data at each lag period to extract the spatial features. These spatial features are then aggregated over time (using averaging) to obtain a spatial representation G. Moreover, the LSTM network is used to directly model the original input data to extract temporal features L. The spatial and temporal representations G and L are then concatenated and passed through two layers of MLP to generate the final prediction variables. Due to the limited sample size, no gating mechanisms (e.g., GLU) are introduced in

https://doi.org/10.7441/joc.2026.03.01

the parallel model to avoid excessive model complexity. **(4) Serial TCN–GCN–TCN Model:** In this model, the TCN is used to extract the temporal features of the financial risk characteristics across cities. The resulting temporal features are then aggregated spatially using the GCN model. Subsequently, the TCN model is again applied to capture the temporal dynamics of the spatially aggregated features. The final predictions are made through an MLP layer.

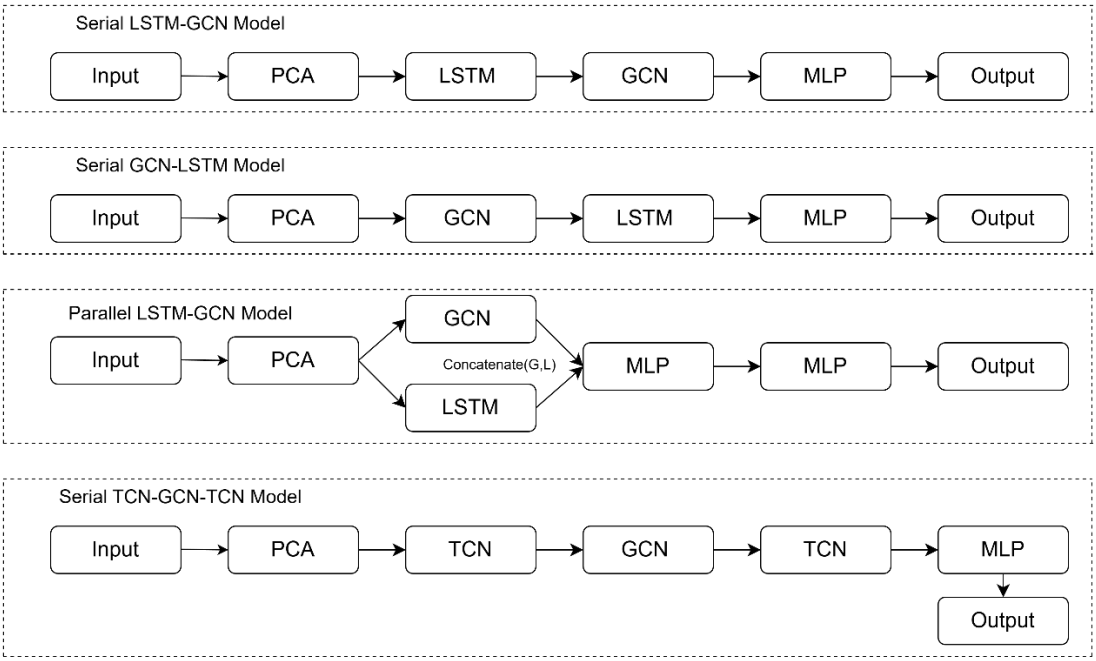


Fig. 1 Design of urban financial risk prediction models based on spatiotemporal graph neural networks. Source: own research

4.2.3 Construction of the adjacency matrix

In the GCN framework, the adjacency matrix A defines the spatial relationships among cities. This study considers five methods for constructing the adjacency matrix. The first four are fixed matrices based on external information, whereas the fifth is a trainable adjacency matrix.

(1) Distance-based adjacency matrix： The adjacency matrix based on geographical distances between cities is the most common construction method. We define the adjacency matrix A as follows:

$$A_{ij} = \begin{cases} 1, & if\ j \in NN_{num_c}(i) \\ 0, & otherwise \end{cases} \tag{26}$$

where $NN_{num_c}(i)$ denotes the index set of the num_c cities with the smallest geographical distances d_{ij}^2 in the i-th row.

(2) Economic gravity adjacency matrix: In the economic gravity model (Wu et al., 2025), the economic gravity weight w_{ij} between two cities is calculated as follows:

$$w_{ij} = \frac{\widehat{GDP}_i \times \widehat{GDP}_j}{\hat{d}_{ij}^2} \tag{27}$$

https://doi.org/10.7441/joc.2026.03.01

where $\widehat{GDP_i}$ and $\widehat{GDP_j}$ are the standardized GDP values, and $\hat{d}_{ij}^2$ is the standardized geographical distance between cities. Standardization uses value/min (value). Subsequently, based on w_{ij}, A_{ij} is calculated using Equation (26).

(3) Financial risk spatial association matrix: According to Shen et al. (2019) and Ouyang & Xiong (2023), the financial risk, population size, economic volume, and geographical distance of a city jointly determine the spatial association network of financial risk. The calculation of the risk spatial association matrix element is as follows:

$$r_{ij} = con_{ij} \frac{\sqrt[3]{Risk_i \cdot POP_i \cdot GDP_i}\sqrt[3]{Risk_j \cdot POP_j \cdot GDP_j}}{\left(\frac{d_{ij}}{PGDP_i - PGDP_j}\right)^2}, con_{ij} = \frac{Risk_i}{Risk_i + Risk_j} \quad (28)$$

where $Risk_i, POP_i, GDP_i,$ and $PGDP_i$ represent the financial risk, population, GDP, and per capita GDP of city i, respectively, and d_{ij} is the geographical distance between cities i and j. The spatial contagion effect between cities i and j is then determined as follows:

$$A_{ij} = \begin{cases} 1, & r_{ij} > m_i \\ 0, & otherwise \end{cases} \quad (29)$$

where m_i is the average risk value of city i.

(4) Similarity-based adjacency matrix: In this method, the financial risk similarity ρ_{ij} between cities i and j is first computed, typically using Pearson correlation coefficients. The adjacency matrix is then constructed based on a predefined threshold p as follows:

$$A_{ij} = \begin{cases} 1, & \rho_{ij} > p \\ 0, & otherwise \end{cases} \quad (30)$$

where the threshold p can be optimized appropriately.

(5) Trainable adjacency matrix: Unlike fixed matrices, the trainable adjacency matrix is treated as a learnable parameter, similar to model weights and biases. The adjacency matrix is randomly initialized and updated through backpropagation during model training. This allows the model to learn data-driven spatial dependence among cities rather than relying exclusively on predefined spatial structures.

5 EMPIRICAL RESULTS

5.1 Spatiotemporal evolution of urban financial risk

5.1.1 Spatial distribution of urban financial risk

Based on data from 2008 to 2023, this study calculates the level of urban financial risk for each city using Equation (9) (Tab.3) and visualizes the spatial distribution in Fig. 2, where darker colors indicate higher levels of urban financial risk. According to Tab.3 and Fig. 2, several key findings can be summarized.

First, significant inter-provincial heterogeneity is observed. The Anhui urban cluster exhibits the highest overall urban financial risk, whereas Jiangsu shows the lowest risk level. Cities in Zhejiang and Shanghai generally fall within the medium-risk range.

https://doi.org/10.7441/joc.2026.03.01

Second, clear spatial clustering patterns emerge in the distribution of urban financial risk. High-risk cities are primarily concentrated in peripheral areas of the YRD. These spatial patterns may reflect potential "risk spillover" or "spatial dependence" among cities, although they may result from shared macroeconomic shocks rather than direct contagion effects.

More specifically, the southwest of Anhui forms a "high-risk cluster," where Chizhou, Anqing, Tongling, and Xuancheng together constitute the core area with the highest urban financial risk in the region. In southern Zhejiang, a clear "risk hotspot" can be observed, with Wenzhou (ranked 7th), Taizhou (9th), and Jinhua (5th) forming a triangular pattern of relatively high financial risk. By contrast, Jiangsu presents a "north–south divergence" in urban financial risk. Cities such as Suzhou, Wuxi, and Changzhou—supported by developed manufacturing industries, high-end service sectors, and relatively advanced financial systems—form a "low-risk triangle." Moreover, Yancheng in northern Jiangsu ranked 6th in 2023, indicating comparatively higher financial risk within the province.

Overall, these results reveal pronounced regional disparities and spatial clustering in the distribution of urban financial risk across the YRD.

Tab.3 – Dynamic comprehensive evaluation of urban financial risk in the Yangtze River Delta urban agglomeration (2008–2023). Source: own research

Cities in Anhui	**Anqing**	**Chizhou**	**Tongling**	**Xuancheng**	**Wuhu**	**Ma'anshan**	**Chuzhou**	**Hefei**	
UFR	0.5947	0.6026	0.5707	0.5615	0.4901	0.5244	0.5159	0.4823	
Ranking	2	1	3	4	16	8	12	21	
Cities in Zhejiang	**Taizhou (ZJ)**	**Zhoushan**	**Jinhua**	**Shaoxing**	**Huzhou**	**Jiaxing**	**Wenzhou**	**Ningbo**	**Hangzhou**
UFR	0.5238	0.4613	0.5524	0.4879	0.5165	0.489	0.5435	0.4555	0.5118
Ranking	9	24	5	19	11	17	7	25	14
Cities in Jiangsu	**Taizhou (JS)**	**Zhenjiang**	**Yangzhou**	**Yancheng**	**Nantong**	**Suzhou**	**Changzhou**	**Wuxi**	**Nanjing**
UFR	0.4956	0.5168	0.4875	0.5492	0.4822	0.4428	0.4624	0.4339	0.4879
Ranking	15	10	20	6	22	26	23	27	18
Shanghai	**Shanghai**								
UFR	0.5152								
Ranking	13								

Note: UFR stands for urban financial risk.

https://doi.org/10.7441/joc.2026.03.01

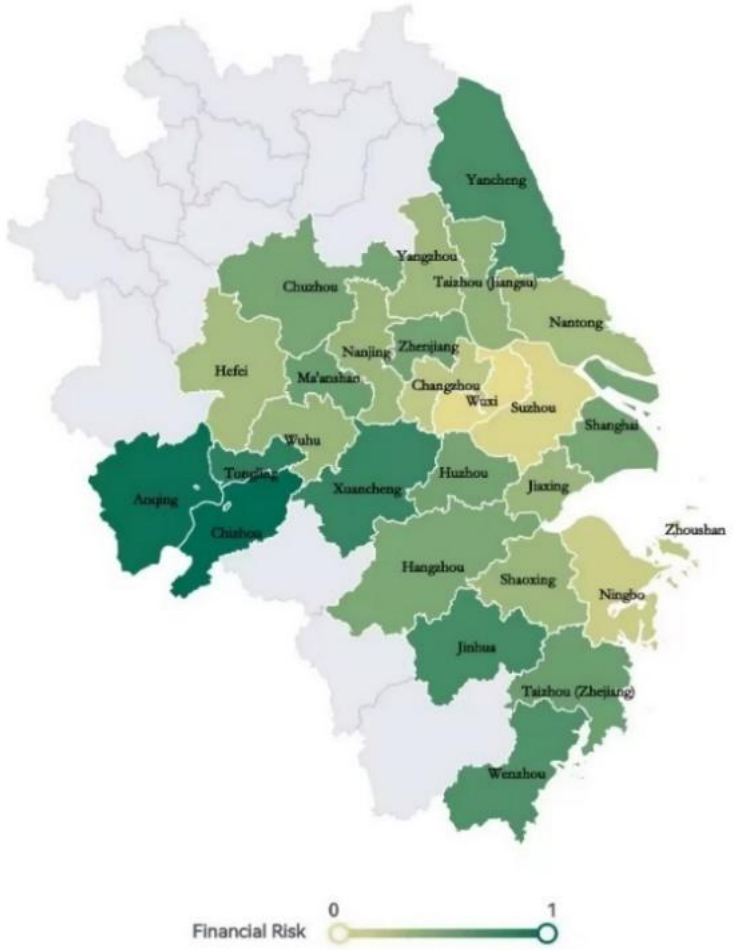


Fig. 2 Spatial distribution of urban financial risk in the Yangtze River Delta urban agglomeration (2008–2023). Source: own research

Based on Equation (9), urban financial risk can be decomposed into the summed contributions of 12 secondary indicators. Fig. 3 shows a heatmap of the ranked contributions of these indicators across cities, providing a more detailed diagnosis of regional risk sources. The main patterns can be summarized as follows.

(1) Southwest Anhui "high-risk cluster": Chizhou, Anqing, Tongling, and Xuancheng form the highest-risk core area in the YRD. As shown in Fig. 3, macroeconomic risk, banking system risk, and government finance and debt risk contribute strongly to overall urban financial risk, whereas real estate risk remains relatively moderate. Persistent population outflows toward nearby developed cities such as Hefei, Hangzhou, and Nanjing weaken local economic fundamentals. Strengthening regional cooperation and improving industrial absorption capacity would help alleviate fiscal and financial pressures.

(2) Southern Zhejiang "risk hotspot": Jinhua, Wenzhou, and Taizhou constitute a regional risk hotspot. Jinhua and Wenzhou show relatively low macroeconomic risk but higher banking, real estate, and fiscal-debt risks. Taizhou displays higher macroeconomic and fiscal risks but lower banking and real estate risks. A common feature across the three cities is the strong contribution of government finance and debt risk. The dominance of low-value-added manufacturing, combined with active informal financing and expansion of local government

https://doi.org/10.7441/joc.2026.03.01

financing vehicles, increases fiscal and financial vulnerabilities. Policy priorities include financial structure optimization, strengthened fiscal supervision, and industrial upgrading.

(3) North–South divergence in Jiangsu Province: Suzhou, Wuxi, and Changzhou form a "low-risk area" supported by advanced manufacturing, strong service sectors, and relatively stable financial systems. Nevertheless, Suzhou shows pressure from high housing price-to-income ratios, while Changzhou faces environmental constraints. By contrast, Yancheng exhibits relatively higher urban financial risk, primarily driven by macroeconomic and fiscal-debt factors. Differentiated policy responses are therefore required to address city-specific risk sources.

(4) Shanghai: Shanghai maintains a moderate level of urban financial risk. As China's financial center, Shanghai benefits from strong economic fundamentals and relatively controlled government debt risk. However, banking system risk and real estate market risk remain comparatively prominent. Targeted financial supervision and real estate risk management are therefore crucial to maintain long-term financial stability.

Overall, the YRD exhibits clear provincial heterogeneity and spatial clustering in urban financial risk. Effective risk mitigation requires differentiated governance strategies and stronger cross-regional coordination in financial supervision.

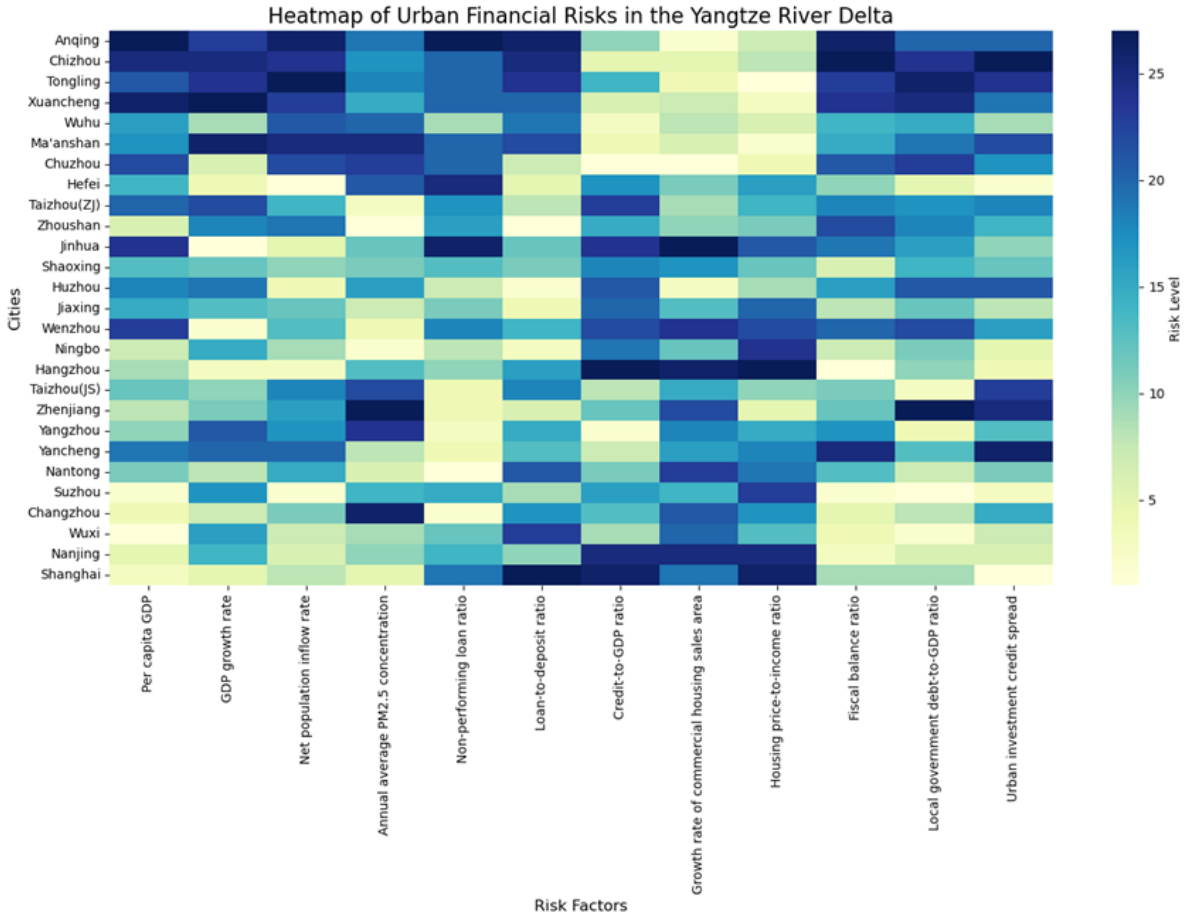


Fig. 3 Heatmap of the ranked contributions of the 12 indicators to urban financial risk in the Yangtze River Delta urban agglomeration. Source: own research

https://doi.org/10.7441/joc.2026.03.01

5.1.2 Temporal evolution of urban financial risk

Annual urban financial risk scores for each city are computed using Equation (31) as follows:

$$r_i(t_k) = \sum_{j=1}^{m} \omega_j \, x_{ijk}^{**} \tag{31}$$

where ω_j represents the dynamic indicator weight, derived from Equations (14) and (15).

To examine the long-term evolution of urban financial risk, the Cox–Stuart test is applied to the time series of each city over the period 2008–2023. The hypotheses are defined as follows:

$$H_0: \text{no monotonic trend} \quad H_1: \text{monotonic trend}$$

The corresponding *p* values for the 27 cities in the YRD are shown in Fig. 4. When the *p* value is below the significance level (e.g., 0.05), the null hypothesis is rejected, indicating a statistically significant monotonic trend in urban financial risk.

As shown in Fig. 4, the long-term evolution of urban financial risk can be classified into three groups.

(1) No significant trend: Shanghai, Suzhou, Nantong, Yancheng, Zhenjiang, Taizhou, Huzhou, Jinhua, Chuzhou, Ma'anshan, Tongling, Chizhou, and Anqing show no clear upward or downward trend.

(2) Significant trend: Yangzhou, Zhoushan, Hefei, Wuhu, and Xuancheng exhibit statistically significant increasing or decreasing trends in urban financial risk.

(3) Weak or ambiguous trend: Nanjing, Wuxi, Changzhou, Hangzhou, Ningbo, Wenzhou, Jiaxing, Shaoxing, and Taizhou show some variation, but no strong or consistent trend is identified.

To further assess the magnitude of change, the risk change rate is defined as follows:

$$\frac{\text{Average financial risk (2016–2023)} - \text{Average financial risk (2008–2015)}}{\text{Average financial risk (2008–2015)}} \tag{32}$$

Among the 27 cities, only Tongling exhibits a positive change rate, whereas all other cities show negative values. This indicates that, overall, urban financial risk in the YRD has declined over time.

https://doi.org/10.7441/joc.2026.03.01

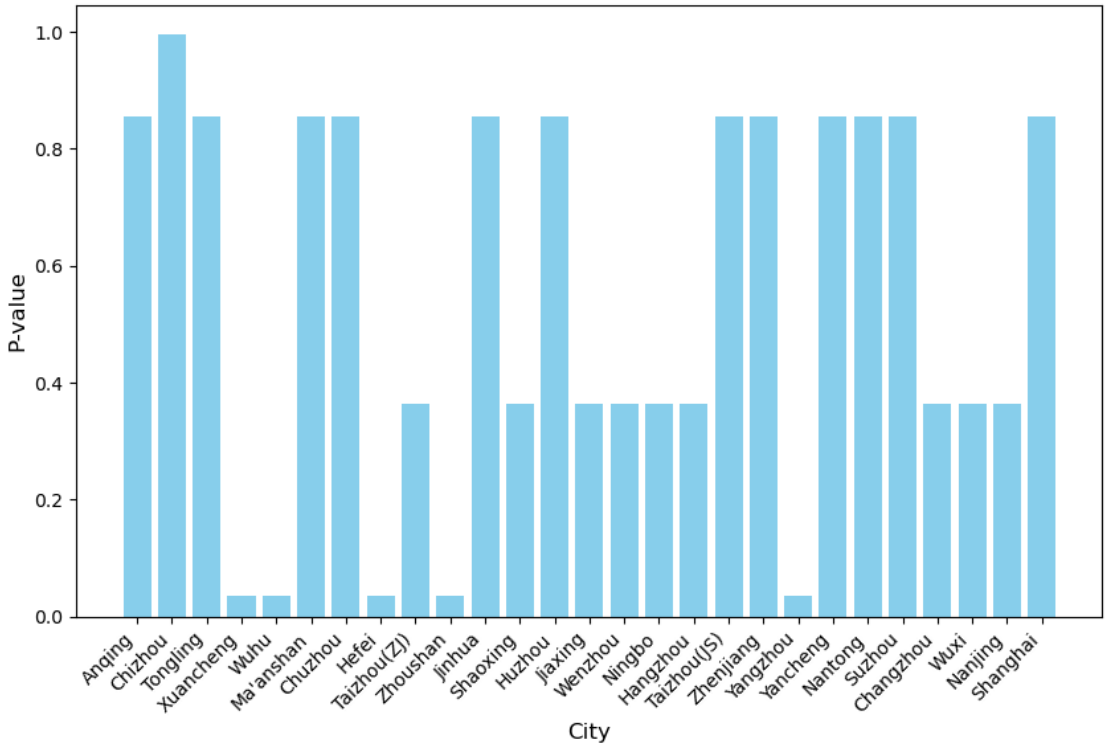


Fig. 4 *p* values from the Cox–Stuart trend test for urban financial risk in the Yangtze River Delta urban agglomeration. Source: own research

Subsequently, this study ranks urban financial risk for each city in the YRD annually and examines the evolution of these rankings over time. Compared with absolute risk levels, ranking analysis focuses on relative risk dynamics, which helps reduce the influence of common macroeconomic shocks and highlights intra-regional differences in urban financial risk.

Fig. 5 reports the change rate of urban financial risk rankings for the 27 cities, defined as follows:

$$\frac{\text{Average rank (2016–2023)} - \text{Average rank (2008–2015)}}{\text{Average rank (2008–2015)}} \tag{33}$$

A negative value indicates an improvement in the relative risk position, whereas a positive value indicates deterioration. Fig. 6 shows a heatmap of the temporal evolution of urban financial risk rankings from 2008 to 2023 across Anhui, Zhejiang, Jiangsu, and Shanghai. Smaller ranking values correspond to higher urban financial risk.

Combining Figs. 5 and 6, several regional patterns emerge.

(1) Anhui cluster: Wuhu, Chuzhou, and Hefei show clear improvements in urban financial risk rankings. By contrast, Anqing, Chizhou, Tongling, and Ma'anshan exhibit noticeable deterioration, whereas Xuancheng remains persistently among the higher-risk cities despite only moderate ranking changes.

(2) Zhejiang cluster: Zhoushan, Huzhou, Jiaxing, and Ningbo demonstrate substantial improvements in urban financial risk rankings. Hangzhou shows only slight improvement and remains at a relatively high-risk level. By contrast, Taizhou, Jinhua, and Wenzhou experience

https://doi.org/10.7441/joc.2026.03.01

notable deterioration, whereas Shaoxing shows mild worsening but remains within a relatively low-risk range.

(3) Jiangsu cluster: Yancheng exhibits the most pronounced deterioration in urban financial risk ranking. Taizhou and Zhenjiang show moderate upward pressure. By contrast, Yangzhou, Nantong, Suzhou, Changzhou, and Wuxi improve significantly, whereas Nanjing shows a modest improvement.

(4) Shanghai: Shanghai's urban financial risk ranking shows a modest but statistically insignificant improvement, indicating relatively stable risk conditions over the sample period.

Overall, the ranking dynamics reveal substantial heterogeneity in the evolution of urban financial risk across cities in the YRD, indicating that financial risk governance requires differentiated strategies across regions.

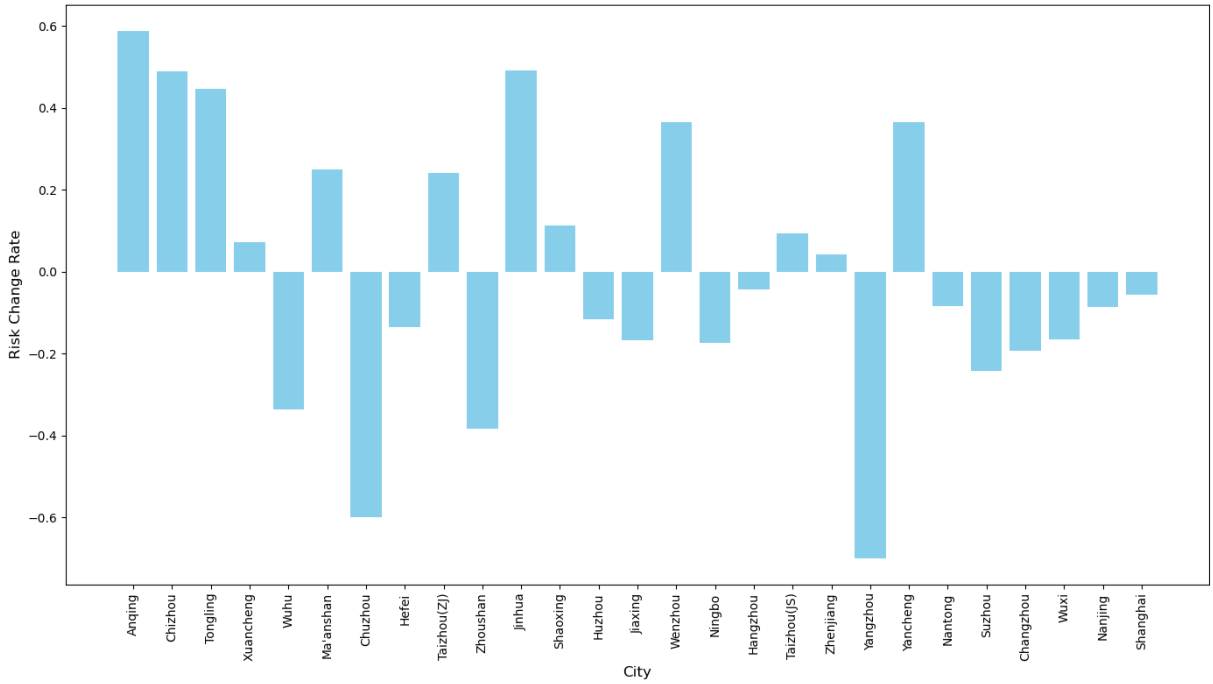


Fig. 5 Rate of change in urban financial risk rankings in the Yangtze River Delta (2008–2023). Source: own research

https://doi.org/10.7441/joc.2026.03.01

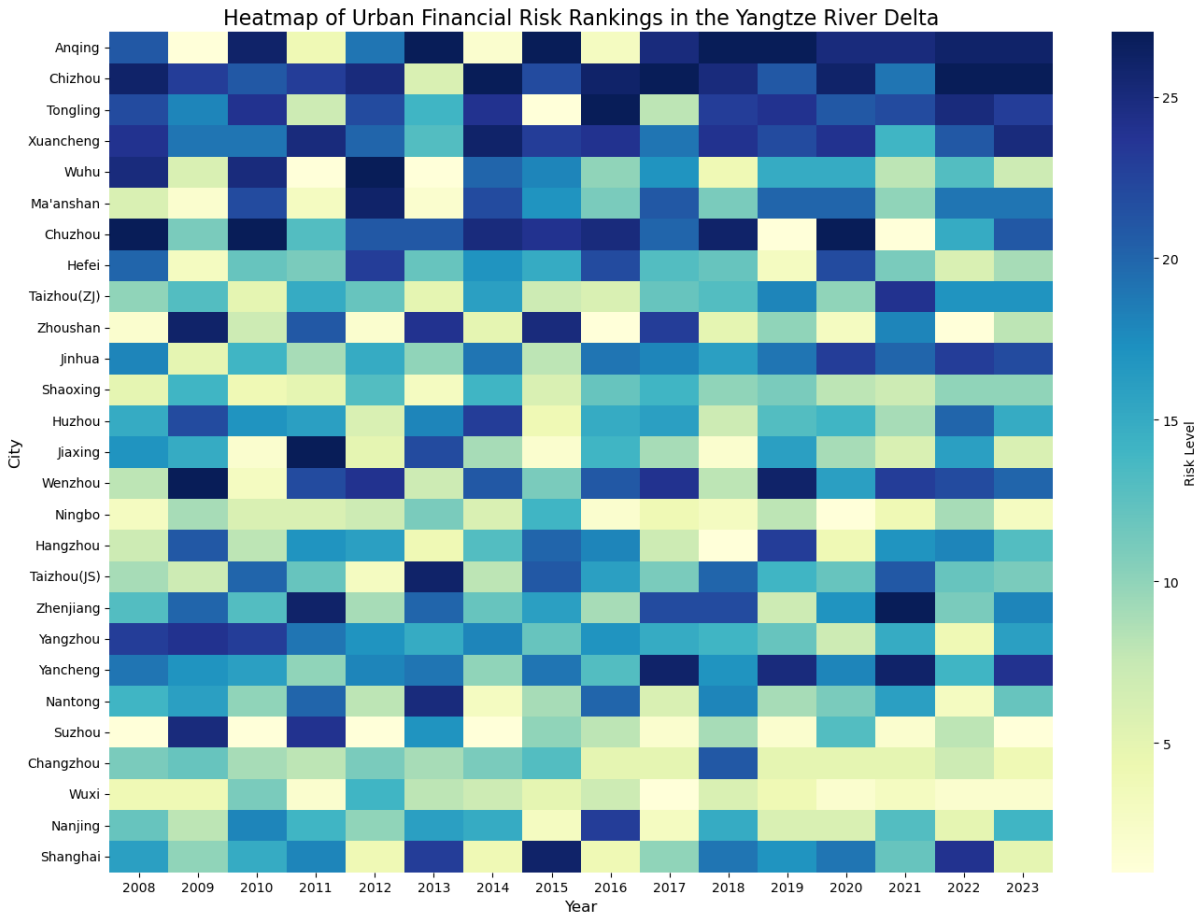


Fig. 6 Temporal evolution of urban financial risk rankings in the Yangtze River Delta (2008–2023). Source: own research

5.2 Forecasting performance and model evaluation

This study aimed to develop urban financial risk prediction models and evaluates their performance and generalization ability using the 27 cities of the YRD in 2023 as a test set.

Algorithm Steps:

Step 1: Validation set selection and hyperparameter optimization

1) A candidate validation set $V = \{2018,2019,2020,2021,2022\}$ is defined.

2) For each year $v \in V$, it is used as the validation set, and the remaining years (excluding the test year, 2023) are used as the training set.

3) Using the Optuna framework, Bayesian optimization is performed to minimize the Mean Squared Error (MSE) on the validation set, selecting the year v^* and its corresponding optimal hyperparameter configuration that minimizes the MSE.

Note: The validation set spans 2018–2022 to cover different macroeconomic environments before and after the pandemic, ensuring comparability with the 2023 test set.

Step 2: Final model training and testing

https://doi.org/10.7441/joc.2026.03.01

1) The optimal validation year v^* and hyperparameters are fixed.

2) The model is retrained using data from 2008 to 2022 (excluding the validation year v^*).

3) The performance of the model is evaluated on the training set and the 2023 test set using metrics such as the coefficient of determination (R^2).

Step 3: Repeated experiments and robustness evaluation

1) Under the optimal hyperparameter configuration, each spatiotemporal model is trained 19 times.

2) The median R^2 of the test set results is used as the final goodness-of-fit indicator, and the sample standard deviation is used to assess the uncertainty and stability of the predictions of the model.

3) Robustness check: An additional test set using data from the 27 cities in 2022 is created to assess the robustness of the model across different time periods.

5.2.1 Experimental setup and hyperparameter optimization

The model was developed and trained in Python 3.8 with TensorFlow 2.7.0. The specific experimental settings are as follows:

1) PCA for dimensionality reduction: Given the limited sample size of 405 data points, PCA was applied to reduce the original 31 input features. A total of 18 principal components were retained, ensuring that the cumulative variance contribution was at least 92%, effectively removing redundancy and emphasizing key risk factors.

2) Time series lag setting: A lag of 2 years was used for the time series modeling. This lag is appropriate given that some features are expressed as year-on-year growth rates, which effectively capture the phased changes in urban financial risk and its "acceleration" characteristics.

3) Regularization and hyperparameter optimization: To mitigate overfitting under small sample conditions, a dropout mechanism was introduced in each network module, and L2 regularization was applied to all model parameters except the trainable adjacency matrix. Due to limited sample size, early stopping was not employed, as it showed instability in preliminary experiments. Hyperparameters were optimized using **Optuna**, with the specific search range and settings detailed in Tab.4.

Tab.4 – Optuna hyperparameter optimization settings. Source: own research

Models	Units	Layers	Dropout probability	L2 regularization	Learning rate	Validation set
LSTM	[4,128]	[1,2]	[0.01,0.5]	[1e−5, 1e−2]	[1e−5, 1e−2]	[8,12]
Two-Layer LSTM	[4,128]	[1,2]	[0.01,0.5]	[1e−5, 1e−2]	[1e−5, 1e−2]	[8,12]
Serial LSTM–GCN	[4,128]	1	[0.01,0.5]	[1e−5, 1e−2]	[1e−5, 1e−2]	[8,12]
Serial GCN–LSTM	[4,128]	1	[0.01,0.5]	[1e−5, 1e−2]	[1e−5, 1e−2]	[8,12]
Parallel LSTM–GCN	[4,128]	1	[0.01,0.5]	[1e−5, 1e−2]	[1e−5, 1e−2]	[8,12]
Serial TCN–GCN–TCN	[4,128]	1	[0.01,0.5]	[1e−5, 1e−2]	[1e−5, 1e−2]	[8,12]

https://doi.org/10.7441/joc.2026.03.01

Note 1: Each module in the spatiotemporal neural network model (e.g., the LSTM–GCN model) contains multiple hyperparameter settings. For instance, the LSTM module has its own units parameter, and the GCN module has a separate units parameter. To ensure consistency, this study adopts the same hyperparameter range for the number of units across all modules.

Note 2: [8, 12] denotes the selection of one year as the validation set within the period 2018–2022. In particular, validation set "12" refers to using data from 2022 as the validation set, which includes financial risk data for 27 cities.

5.2.2 Comparison of fixed and trainable adjacency matrices

Tab.5 presents the R^2 median and model uncertainty from 19 training runs for four fixed adjacency matrices and the trainable adjacency matrix in the serial LSTM–GCN model. Among the fixed adjacency matrices, the similarity-based adjacency matrix performed best on the training and test sets, with R^2 medians of 0.6055 and 0.1459, respectively. However, the overall performance was still moderate. This suggests that fixed adjacency matrices based on geography, economics, and financial significance did not significantly improve the prediction performance of the urban financial risk model.

The study further proposes treating the adjacency matrix as a trainable parameter, akin to the weights of the model. In the serial LSTM–GCN model, using the trainable adjacency matrix improved the R^2 medians for the training and test sets, reaching 0.9673 and 0.4131, respectively, compared with the fixed matrices. This improvement was significant, with model uncertainty remaining relatively low.

As a result, the trainable adjacency matrix will be used in subsequent analyses to construct the spatiotemporal neural network model and conduct robustness testing.

Tab.5 – Comparison of prediction performance for different adjacency matrices in serial LSTM–GCN. Source: own research

Adjacency matrix	Distance-based	Economic gravity model	Financial risk spatial network	Similarity matrix	Trainable adjacency matrix
Training set R^2 median	0.3728	0.2258	0.2661	0.6055	**0.9673**
Model uncertainty	0.0222	0.0162	0.0302	0.0293	0.0027
Test set R^2 median	0.1218	0.0312	0.0831	0.1459	**0.4131**
Model uncertainty	0.0228	0.0192	0.0351	0.0344	0.0582

Note: For the distance-based and economic gravity models, $num_c = 2$, and for the similarity matrix, the threshold $p = 0.94$.

5.2.3 Performance comparison of spatiotemporal models

The study first constructed the GCN model using a trainable adjacency matrix and then evaluated the performance of four spatiotemporal architectures, along with benchmark models (LSTM and Two-Layer LSTM), using 2023 data as the test set.

As reported in Tab.6, the Two-Layer LSTM improved the training performance compared with the single-layer LSTM, increasing the median training R^2 from 0.8468 to 0.8792, indicating that deeper temporal modeling enhances the fitting ability of the baseline model.

Among the spatiotemporal models, all four architectures achieved substantially higher training R^2 values than the benchmark models. In particular, the Serial GCN–LSTM model achieved the highest training R^2 (0.9885), followed by Serial LSTM–GCN (0.9673) and Serial TCN–GCN–TCN (0.9629), indicating that incorporating spatial information can significantly enhance the fitting capability of the model.

https://doi.org/10.7441/joc.2026.03.01

However, differences become more apparent when examining the test set results. As presented in Tab.6, the Serial LSTM–GCN model achieved the highest test R^2 (0.4131), outperforming the LSTM (0.2582) and the Two-Layer LSTM (0.3896). The Serial GCN–LSTM (0.3857) and Parallel LSTM–GCN (0.3740) models achieved performance close to the Two-Layer LSTM benchmark, whereas the Serial TCN–GCN–TCN model (0.2751) showed relatively weaker predictive performance.

Tab.6 R^2 values of spatiotemporal models with 2023 as the test set. Source: own research

Model	LSTM	Two-Layer LSTM	Serial LSTM–GCN	Serial GCN–LSTM	Parallel LSTM–GCN	Serial TCN–GCN–TCN
Training set R^2 median	0.8468	0.8792	0.9673	**0.9885**	0.9338	0.9629
Model uncertainty	0.0142	0.0049	0.003	0.0025	0.0112	0.0131
Test set R^2 median	0.2582	0.3896	**0.4131**	0.3857	0.3740	0.2751
Model uncertainty	0.0532	0.0298	0.0582	0.0614	0.0553	0.0868

To further evaluate predictive accuracy, RMSE results reported in Tab.7 provide additional evidence. The Serial LSTM–GCN model achieved the lowest test RMSE (0.2635), slightly outperforming the LSTM (0.2726) and Two-Layer LSTM (0.2735). By contrast, the Serial GCN–LSTM (0.2929) and Serial TCN–GCN–TCN (0.2864) models produced larger prediction errors, whereas the Parallel LSTM–GCN model (0.2761) performed similarly to the benchmark models.

Overall, these results indicate that incorporating spatial dependency through graph structures can improve predictive performance when appropriately integrated with temporal modeling. In particular, the Serial LSTM–GCN architecture demonstrates optimal balance between fitting ability and predictive accuracy for the 2023 test set, indicating that modeling temporal dynamics first and then capturing spatial spillovers can effectively improve forecasting performance for urban financial risk in the YRD.

Tab.7 RMSE values of spatiotemporal models with 2023 as the test set. Source: own research

Model	LSTM	Two-Layer LSTM	Serial LSTM–GCN	Serial GCN–LSTM	Parallel LSTM–GCN	Serial TCN–GCN–TCN
Training set RMSE median	0.1128	0.0983	**0.0408**	0.1261	0.0932	0.0920
Model uncertainty	0.0014	0.0039	0.0074	0.0052	0.0049	0.0038
Test set RMSE median	0.2726	0.2735	**0.2635**	0.2929	0.2761	0.2864
Model uncertainty	0.0067	0.0107	0.0101	0.0132	0.0209	0.0145

5.2.4 Robustness analysis

To further verify the robustness of the models, the study used 2022 data as an alternative test set, with the validation period ranging from 2018 to 2021.

As presented in Tab.8, the training results differ from those observed in the 2023 test setting. In the training set, the Parallel LSTM–GCN (0.9622) and Serial TCN–GCN–TCN (0.9489) models achieved the highest R^2 values, indicating stronger fitting performance than both benchmark models. By contrast, the Serial GCN–LSTM model (0.8414) exhibited a relatively weaker training fit among the spatiotemporal architectures.

https://doi.org/10.7441/joc.2026.03.01

On the test set, however, the ranking of the model changes. The Serial GCN–LSTM model achieved the highest R^2 (0.6690), followed by Serial LSTM–GCN (0.6190) and Parallel LSTM–GCN (0.6181). All four spatiotemporal models achieved higher predictive performance than the single-layer LSTM (0.5697) and the Two-Layer LSTM (0.5891), indicating that incorporating spatial structure can improve prediction performance under different temporal settings.

Overall, results based on the 2022 test set confirm the robustness of the spatiotemporal modeling framework, although the relative performance of individual architectures varies across test periods. This suggests that while spatiotemporal neural networks can effectively capture temporal dynamics and spatial interactions in urban financial risk, differences in time periods and evolving risk characteristics across cities may lead to variations in model performance.

Tab. 8 R^2 values of spatiotemporal models with 2022 as the test set. Source: own research

Model	LSTM	Two-Layer LSTM	Serial LSTM–GCN	Serial GCN–LSTM	Parallel LSTM–GCN	Serial TCN–GCN–TCN
Training set R^2 median	0.9155	0.8585	0.8585	0.8414	0.9622	0.9489
Model uncertainty	0.0047	0.0129	0.0131	0.0147	0.007	0.0093
Test set R^2 median	0.5697	0.5891	0.6190	0.6690	0.6181	0.6053
Model uncertainty	0.0381	0.0560	0.1137	0.0722	0.1107	0.03812

6 CONCLUSION

Amid multiple challenges—including the COVID-19 pandemic, trade frictions, real estate market adjustments, and population aging—China's economy has entered a stage of high-quality and sustainable development. In this context, effective management of urban financial risk has become increasingly crucial for maintaining regional stability and supporting long-term economic resilience. As one of the most dynamic regions in China, the YRD exhibits a complex and evolving pattern of urban financial risk, making systematic measurement and forecasting particularly essential.

This study focuses on the measurement, spatiotemporal evolution, and forecasting of urban financial risk, addressing key limitations in existing city-level research. The main findings are summarized as follows.

6.1 Measurement and spatiotemporal evolution of urban financial risk

First, a multidimensional urban financial risk measurement framework is constructed, incorporating four key dimensions: macroeconomic risk, banking system risk, real estate market risk, and government finance and debt risk. The framework is further enriched by introducing $PM_{2.5}$ concentration to capture environmental influences and credit spreads of local government financing vehicles to reflect implicit debt risk. Proxy variables are used to address data limitations in banking risk across cities.

Based on this framework, a dynamic weighting approach with an "acceleration effect" is applied to examine the evolution of urban financial risk in the YRD from 2008 to 2023. Results reveal clear inter-provincial heterogeneity and spatial clustering. Anhui exhibits relatively higher risk levels, Zhejiang and Shanghai remain at moderate levels, and Jiangsu shows comparatively lower risk, forming a broad pattern of regional differentiation.

https://doi.org/10.7441/joc.2026.03.01

At the city level, distinct spatial clusters are identified. Southwestern Anhui forms a "high-risk cluster," whereas parts of southern Zhejiang constitute a "risk hotspot." However, the underlying drivers differ across cities, including fiscal pressure, industrial structure, and real estate dynamics.

These spatial patterns should be interpreted with caution. The observed clustering reflects spatial dependence in urban financial risk, which may arise from economic linkages or shared external shocks, rather than direct causal contagion.

From a temporal perspective, cities can be grouped into three categories: those with stable risk levels, those with significant upward or downward trends, and those with high volatility but no clear trend. Combined analysis of risk change rates and ranking dynamics suggests that although overall urban financial risk has declined in recent years, substantial cross-city disparities persist.

6.2 Spatiotemporal forecasting of urban financial risk

Building on measurement results, this study develops a forecasting framework for urban financial risk using 31 indicators and four spatiotemporal neural network architectures: Serial LSTM–GCN, Serial GCN–LSTM, Parallel LSTM–GCN, and Serial TCN–GCN–TCN.

Comparisons across different adjacency matrices show that fixed spatial structures do not significantly improve model performance. By contrast, treating the adjacency matrix as a trainable parameter enhances predictive accuracy without increasing uncertainty.

Empirical results indicate that incorporating spatial information improves model performance relative to benchmark models. On the 2023 test set, the Serial LSTM–GCN model achieves optimal performance in terms of R^2 and RMSE, whereas other spatiotemporal models show comparable but less consistent results.

Robustness tests using 2022 data confirm the effectiveness of the spatiotemporal framework, although model rankings vary across test periods. This suggests that model performance depends on evolving temporal dynamics and interurban relationships, and no single architecture consistently dominates across all scenarios.

Overall, results highlight the importance of integrating spatial dependence into temporal models for forecasting urban financial risk.

6.3 Limitations and future research

This study has several limitations. The relatively small sample size limits the application of techniques such as early stopping and transfer learning. Future research should explore spatiotemporal data augmentation (Zhou et al., 2025) to improve model generalization.

Methodologically, future work should improve feature fusion by introducing gating mechanisms or modular architectures to better capture temporal and spatial heterogeneity.

In addition, future research should extend the analysis to urban competitiveness, which is not directly examined in this study. This includes developing a clear evaluation framework, integrating competitiveness-related indicators, and constructing joint models of financial risk and competitiveness. Future research should explore the relationship between urban financial

https://doi.org/10.7441/joc.2026.03.01

risk and competitiveness dynamics, as well as incorporate institutional and governance-related factors using approaches such as text mining.

Funding

This research was supported by the Zhejiang Provincial Social Science Planning Project (Special Topic on the Interpretation of the Spirit of the Third Plenary Session of the 20th CPC Central Committee and the Fifth Plenary Session of the 15th Zhejiang Provincial Committee, Grant No. 25QHJS033YB), and the China Postdoctoral Science Foundation (General Program, Grant No.2024M752688).

References

1. Ahn, J.J., Oh, K.J., Kim, T.Y., & Kim, D.H. (2011). Usefulness of Support Vector Machine to develop an early warning system for financial crisis. *Expert Systems with Applications*, 38 (4), 2966-2973. https://doi.org/10.1016/j.eswa.2010.08.085
2. Akhtaruzzaman, M., Boubaker, S., & Sensoy, A. (2021). Financial contagion during COVID-19 crisis. *Finance Research Letters*, 38, 101604-101604. https://doi.org/10.1016/j.frl.2020.101604
3. Allen, F., Babus, A., & Carletti, E. (2012). Asset commonality, debt maturity and systemic risk. *Journal of Financial Economics*, 104 (3), 519-534. https://doi.org/10.1016/j.jfineco.2011.07.003
4. Arbia, G., Bramante, R., Facchinetti, S., & Zappa, D. (2018). Modeling inter-country spatial financial interactions with Graphical Lasso: An application to sovereign co-risk evaluation. *Regional Science and Urban Economics*, 70 (C), 72–79. https://doi.org/10.1016/j.regsciurbeco.2018.02.006
5. An, S.F., Gao, X.Y., An, F., & Wu, T. (2025) Early warning of regime switching in a complex financial system from a spillover network dynamic perspective. *Iscience*, 28 (3), 111924. https://doi.org/10.1016/j.isci.2025.111924
6. Bae, K.-H., Karolyi, G. A., & Stulz, R. M. (2003). A new approach to measuring financial contagion. *Review of Financial Studies*, 16 (3), 717–763. https://doi.org/10.1093/rfs/hhg012
7. Beirne, J., & Fratzscher, M. (2013). The pricing of sovereign risk and contagion during the European sovereign debt crisis. *Journal of International Money and Finance,* 34, 60–82. https://doi.org/10.1016/j.jimonfin.2012.11.004
8. Chen, S.D., Li, Z., & Lin, S.H. (2020). The spatial spillover effect of local government debt risk on regional financial risk. *Journal of Xi'an Jiaotong University (Social Science) (in Chinese)* , 40 (6), 33-44. https://doi.org/10.15896/j.xjtuskxb.202006004
9. Chen, S.D., Yang, Y., & Ma, H. (2006). The study of Early-Warning on Chinese financial risk. *The Journal of Quantitative and Technical Economics (in Chinese)*, 23 (7), 36-48. https://doi.org/10.13653/j.cnki.jqte.2006.07.004 .
10. Claessens, S., Dell'Ariccia, G., Igan, D., & Laeven, L. (2010). Cross-country experiences and policy implications from the global financial crisis. *Economic Policy*, 25 (62), 267-293. https://doi.org/10.1111/j.1468-0327.2010.00244.x

11. Chen, M.H., Chen, P., & Xu, C.H. (2026). Interactive stress and synergistic response of ecological security and environmental carrying capacity in the Yangtze River Delta Urban Agglomeration. *Sustainability*, 18 (1), 443. https://doi.org/10.3390/su18010443
12. Dang, Y., Miao, Z.Q., Zhang, T., & Feng, D.F. (2022). Application progress of big data method in systemic financial risk monitoring and early warning. *Journal of Financial Development Research (in Chinese)*, 2, 3-12. https://doi.org/10.19647/j.cnki.37-1462/f.2022.02.001
13. Ding, L., Li, P.T., & Liu, L.X. (2019). Construction and application on China financial stress index. *Statistics and Information Forum (in Chinese)*, 34 (10), 63-72.
14. Ding, S.J., Zhuang, X.J., & Li, W.J. (2019). Inter-sectoral contagion mechanism of regional financial risks and an empirical analysis. *Economic Survey (in Chinese),* 36 (3), 1-8. https://doi.org/10.15931/j.cnki.1006-1096.2019.03.002
15. Feng, L., Dong, H.X., & Hao, J.J. (2016). A study of the evaluation of risk contagion of regional finance based on ESDA—The empirical study of county data of Shandong Province. *Review of Economy Management (in Chinese)*, 32 (1), 135-139. https://doi.org/10.13962/j.cnki.37-1486/f.2016.01.017.
16. Guo, Y.J. (2002). New theory and method of dynamic comprehensive evaluation. *Journal of Management Sciences (in Chinese),* 5 (2), 50-54.
17. Gai, P., & Kapadia, S. (2010). Contagion in financial networks. *Proceedings of the Royal Society A-Mathematical Physical and Engineering Science*s, 466 (2120), 2401-2423. https://doi.org/10.1098/rspa.2009.0410
18. Geng, G., Zhang, Q., Martin, R.V., van Donkelaar, A., Huo, H., Che, H.Z., Lin, T.Z., & He, K.B. (2015). Estimating long-term $PM_{2.5}$ concentrations in China using satellite-based aerosol optical depth and a chemical transport model. *Remote Sensing of Environment*, 166, 262-270. https://doi.org/10.1016/j.rse.2015.05.016
19. Gaigaliene, A., & Jurakovaite, O. (2024). Post global financial crisis multiplex financial network structure investigation for 234 countries. Equilibrium. *Quarterly Journal of Economics and Economic Policy*, 19 (1), 23-57. https://doi.org/10.24136/eq.3023
20. Galesi, A., & Sgherri, S. (2009). Regional financial spillovers across Europe: A Global VAR Analysis. *IMF Working Paper* , 09/23, 1–1. https://doi.org/10.5089/9781451871708.001
21. Gil-Alana, L.A., Abakah, E.J.A., & Abakah, M.K. (2020). Financial stress spillover across Asian countries. *Review of Financial Economics*, 39 (2), 146–162. https://doi.org/10.1002/rfe.1113
22. Giua, M., Pericoli, F.M., & Pierucci, E. (2024). EU cohesion policy and inter-regional risk-sharing: First evidence and lessons learned. *Journal of Common Market Studies*, 62 (1), 142–167. https://doi.org/10.1111/jcms.13483
23. Guesmi, K., Abid, I., Creti, A., & Chevallier, J. (2018). Oil price risk and financial contagion. *Energy Journal*, 39 (2), 97–115. https://doi.org/10.5547/01956574.39.SI2.kgue
24. Guo, Y.J., & Chen, Z.H. (2025). Research on the impact of local government implicit debts on urban economic growth in China. *Sage Open*, 15 (4), 21582440251396154. https://doi.org/10.1177/21582440251396154

https://doi.org/10.7441/joc.2026.03.01

25. Huh, H.S. (2002). GDP growth and the composite leading index: a nonlinear causality analysis for eleven countries. *Economics Letters*, 77 (1), 93-99. https://doi.org/10.1016/S0165-1765(02)00109-X

26. Hua, J.G. (2014). Leading indicators and macroeconomic fluctuation forecasting. *Systems Engineering -Theory & Practice (in Chinese)*, 34 (10), 2539-2545.

27. Hu, M.J., Li, Z.J., Ding, Z.S, Zhou, N.X., Guo, X.Y., & Li, X. (2020). The evolution characteristics and threshold effects of the resource and environmental pressure in the Pan-Yangtze River Delta cities. *Scientia Geographica Sinica (in Chinese)*, 40 (5), 701-709. https://doi.org/10.13249/j.cnki.sgs.2020.05.004

28. Hetzer, L., & Burgoon, B. (2024). Regional crises and European fiscal preferences: How regional Covid-19, economic downturn, and migration shape support for EU risk sharing. *Journal of European Public Policy*, 31 (10), 3093–3127. https://doi.org/10.1080/13501763.2024.2334839

29. Hsiao, C.Y.L., & Morley, J. (2022). Debt and financial market contagion. *Empirical Economics,* 62 (4), 1599–1648. https://doi.org/10.1007/S00181-021-02077-5.

30. Huang, Q.Q., Peng, B.H., Wei, G., & Wan, A.X. (2020). Dynamic assessment and early warning of ecological security: A case study of the Yangtze River urban agglomeration. *Natural Hazards,* 107 (3), 2441–2461. https://doi.org/10.1007/s11069-020-04436-4

31. Huang, X., & Guo, F.Y. (2020). A kernel fuzzy twin SVM model for early warning systems of extreme financial risks. *International Journal of Finance and Economics*, 26 (1), 1459-1468. https://doi.org/10.1002/ijfe.1858

32. Hu, Y.C., Wang, G.J., Gao, W.Y., Lu, G.B., & Uddin, G.S. (2026). Connectedness and systemic importance of global financial markets: A multilayer network perspective. Research in International *Business and Finance*, 84, 103336. https://doi.org/10.1016/j.ribaf.2026.103336

33. Huang, A.S., Chu, M., Cheng, W.X., Wang, G., Guan, P.B., Zhang, L., & Jia, J. (2024). Dynamic evaluation of China's atmospheric environmental pressure from 2008 to 2017: Trends and drivers. *Journal of Environmental Sciences*, 150, 177-187. https://doi.org/10.1016/j.jes.2024.02.017

34. Inekwe, J.N. (2021). Finance and European regional economy. *International Review of Financial Analysis*, 78, 101921. https://doi.org/10.1016/J.IRFA.2021.101921

35. Jung, H.J. (2009). Financial regionalism in east Asia: regional surveillance cooperation and enforcement problem. *Pacific Focus*, 24 (3), 379–401. https://doi.org/10.1111/j.1976-5118.2009.01031.x

36. Kim, T.Y., Oh, K.J., Sohn, I., & Hwang, C.H. (2004). Usefulness of Artificial Neural Networks for early warning system of economic crisis. *Expert Systems with Applications,* 26 (4), 583-590. https://doi.org/10.1016/j.eswa.2003.12.009

37. Kipf, T.N., & Welling, M. (2017). Semi-supervised classification with graph convolutional networks. *Proceedings of International Conference on Learning Representations*, 1-14. https://doi.org/10.48550/arXiv.1609.02907

38. Kumar, M., Moorthy, U., & Perraudin, W. (2003). Predicting emerging market currency crashes. *Journal of Empirical Finance*, 10 (4), 427-454. https://doi.org/10.1016/S0927-5398(02)00068-3

39. Kong, M.Y., & Zhang, S.Q. (2026). Global stock market systemic risk and the asymmetric transmission to Bitcoin's tail dynamics. *Physica A-Statistical Mechanics and Its Applications*, 684, 131241. https://doi.org/10.1016/j.physa.2025.131241

40. Le, C., Dickinson, D., & Le, A. (2022). Sovereign risk spillovers: A network approach. *Journal of Financial Stability*, 60, 101006. https://doi.org/10.1016/j.jfs.2022.101006

41. Li, J.M., Kang, M.L., & Li, Q.Y. (2024). Measurement and evaluation of regional financial risk in China based on entropy weight method. *Economic Forum (in Chinese)*, (2), 98-109.

42. Lin, W.R., Yu, H.J., & Wang, L.G. (2025). A data-driven deep learning approach incorporating investor sentiment and government interventions to predict post-crash stock return in China's A-share market. *Journal of Innovation & Knowledge*. https://doi.org/10.1016/j.jik.2025.100704

43. Li, G.J., Xiong, Z.W., Kou, C.H., & Li, S.S. (2025). Resilience measurement and dynamic evolution of China's provincial financial infrastructure. *Frontiers in Physics*, 13, 1556285. https://doi.org/10.3389/fphy.2025.1556285

44. Ma, C.X., Yang, R.X., Ke, X.L., & Ma, Z.Y. (2022). Construction and optimization of ecological security pattern in Yangtze River Delta based on the perspective of ecological pressure. *Resources and Environment in the Yangtze Basin (in Chinese)*, 31 (1), 135 – 147.

45. Moutinho, V., Almeida, L., Neves, M., & Monteiro, J. (2025). Dynamic cross hedging, conditional co-movements in commodities and financial markets during subprime and sovereign debt crisis: Evidence from China and G7 countries. *Review of Financial Economics*, 43 (3), 261-285. https://doi.org/10.1002/rfe.70000

46. Nag, A., & Mitra, A. (1999). Neural networks and early warning indicators of currency crisis. *Reserve Bank of India Occasional Papers*, 20 (2), 183-205.

47. Ouyang, Z.S., & Xiong, J.Y. (2023). The spillover effect of regional financial risks in China—a study based on social network analysis. *Financial Economic Research (in Chinese)*, 38 (3), 38-50.

48. Ouyang, Z.S., Yang, X.T., & Lai, Y.Z. (2021). Systemic financial risk early warning of financial market in China using attention-LSTM model. *North American Journal of Economics and Finance,* 56, 101383. https://doi.org/10.1016/J.NAJEF.2021.101383.

49. van Donkelaar, A., Hammer, M.S., Bindle, L., Brauer, M., Brook, J.R., & Garay, M.J., et al. (2021). Monthly global estimates of fine particulate matter and their uncertainty. *Environmental Science and Technology,* 55 (22), 15287-15300. https://doi.org/10.1021/ACS.EST.1C05309

50. Park, C.Y., & Mercado, R.V. Jr. (2014). Determinants of financial stress in emerging market economies. *Journal of Banking and Finance,* 45, 199–224. https://doi.org/10.1016/j.jbankfin.2013.09.018.

51. Park, C.Y., & Shin, K. (2020). Contagion through national and regional exposures to foreign banks during the global financial crisis. *Journal of Financial Stability*, 46, 100721. https://doi.org/10.1016/j.jfs.2019.100721

52. Pascha, W. (2007). The role of regional financial arrangements and monetary integration in East Asia and Europe in relations with the United States. *Pacific Review*, 20 (3), 423–446. https://doi.org/10.1080/09512740701461553

53. Parashar, N., Pillai, D., Singh, A.S., & Joshi, A. (2026). Impact of financial market infrastructure: Interconnectedness, spillovers, and systemic resilience in emerging economies. Cogent *Economics & Finance*, 14 (1), 2622216. https://doi.org/10.1080/23322039.2026.2622216

54. Qi, M., Zhang, J.W., Shi, D.Y., Feng, S.Y., & Xu, J. (2025). Systemic risk contagion and bailout effects in the global financial system. *International Review of Economics & Finance*, 102, 104298. https://doi.org/10.1016/j.iref.2025.104298

55. Reinhart, C.M., & Rogoff, K.S. (2009). The aftermath of financial crises. *American Economic Review*, 99 (2), 466-472. https://www.jstor.org/stable/25592442

56. Ren, Y.H., Jiang, J.F., & Ni, Q.S. (2022). A study on financial crisis early warning based on graph neural networks models: a perspective of information spillover among industries. *Statistical Research (in Chinese)*, 39 (8), 141-160. https://doi.org/10.19343/j.cnki.11-1302/c.2022.08.010

57. Ren, Y.H., Chen, X., Chen, H., & Zhu, H.M. (2025). Does inter-industry risk spillover network predict financial crisis? Evidence from a gated graph neural networks approach. *North American Journal of Economics and Finance*, 82, 102565. https://doi.org/10.1016/j.najef.2025.102565

58. Shen, K.R., & Shi, Y. (2022). The patterns, scale measure and risk assessment of local government's implicit liabilities. *Economic Perspectives (in Chinese)*, (7), 16-30.

59. Shen, L., Liu, L.Y., & Li, W.J. (2019). China 's local financial risk spatial correlation network and regional contagion effect: 2009-2016. *Management Review (in Chinese),* 31 (8), 35-48. https://doi.org/10.14120/j.cnki.cn11-5057/f.2019.08.004

60. Tan, Z.M. (2010). Design of regional financial risks' early warning system and it's comprehensive measurement. *Soft Science (in Chinese)*, 24 (3), 69-74. https://doi.org/10.16011/j.cnki.jjwt.2019.05.006

61. Urom, C., Abid, I., Guesmi, K., & Saadi, S. (2026). Contagion, interdependence and global crisis: Evidence from equity markets. *Journal of Financial Stability*, 83, 101508. https://doi.org/10.1016/j.jfs.2026.101508

62. Vega, S.M.H., Patuelli, R., van Voorn, G., & Weinans, E. (2025). Spatial early warning signals to assess economic resilience. *Iscience*, 28 (12), 114097. https://doi.org/10.1016/j.isci.2025.114097

63. Wang, X.K., & Huang, R.L. (2015). Default risk assessment of local government debt based on KMV Model−taking Yangtze River Delta region for example. *Shanghai Economic Research (in Chinese)*, 2015 (4), 62 - 68. https://doi.org/10.19626/j.cnki.cn31-1163/f.2015.04.008

64. Wu, Y.C., Yang, M.A., & Qian, Y.S. (2025). Economic spatial analysis of Lanzhou-Xining urban agglomeration based on modified gravity model. *Science Technology and Industry (in Chinese)*, 25 (2), 153-157.

65. Wan, R., Fan, W.C., & Wang, X.P. (2024). Local government financing vehicle restructuring, implicit government guarantees and debt financing costs: Evidence from the Chinese municipal corporate bond market. *Economic Systems*, 48 (2), 101179.https://doi.org/10.1016/j.ecosys.2024.101179

66. Wang, G.J., Chen, Y., Zhu, Y., & Xie, C. (2024). Systemic risk prediction using machine learning: Does network connectedness help prediction? *International Review of Financial Analysis*, 93, 103147. https://doi.org/10.1016/j.irfa.2024.103147

67. Wang, L., Wang, C.C., Chen, J.Y., & Chang, J.K. (2025). The hidden crowding out effect: How does local government implicit debt pressure influence enterprise productivity in China? *Managerial and Decision Economics*, 46 (1), 502-514.https://doi.org/10.1002/mde.4387

68. Wang, L.X., An, S.F., Dong, Z.L., Dong, X.J., & Li, J.P. (2025). Early warning of regime switching in a financial time series: A heteroskedastic network model. *Plos One*, 0 (10), e0333734. https://doi.org/10.1371/journal.pone.0333734

69. Wei, H.Y., An, F., Gao, X.Y., & Sun, X.T.(2025). Self-dynamics and inter-dynamics network reconstruction for characterizing the systemic risk in stock market. *Chaos Solitons & Fractals*, 201 (3), 117312. https://doi.org/10.1016/j.chaos.2025.117312

70. Xie, T.T., & Li, Y. (2020). Study on regional financial risk measurement in Xinjiang based on entropy method. *Journal of Shihezi University (Philosophy and Social Sciences) (in Chinese)*, 34 (5), 62-69. https://doi.org/10.13880/j.cnki.cn65-1210/c.2020.05.009

71. Xiong, S., Wang, Y., Wang, Y.F., & Wei, Y.S. (2026). Forecasting carbon-coal price co-movement evolution and its implications for emission reduction: An AI-based complex network approach. *Energy*, 348, 140611. https://doi.org/10.1016/j.energy.2026.140611

72. Xu, L.J., Liu, Y.J., Li, X.T., & Zhang, X. (2025). Spillover effect of local government debt on regional financial risk: Evidence from China. *Finance Research Letters*, 87, 108904. https://doi.org/10.1016/j.frl.2025.108904

73. Yi, P.T, Zhou, Y., Guo, Y.J., & Li, W.W. (2016). A dynamic comprehensive evaluation method embodying development tendency. *Operations Research and Management Science (in Chinese)*, 25 (6), 175-180.

74. Yuan，Y. (2022). Analysis of regional financial risk in Guangdong province based on the DCN deep learning model. *Computational Intelligence and Neuroscience*, 2022, 9274737. https://doi.org/10.3390/SYSTEMS10060207

75. Yang, X., Wang, X.Y., Cao, J., Song, L.J. & Huang, C.X. (2024). Can local government implicit debt raise regional financial market spillover? Evidence from China. *Finance Research Letters*, 67 (A), 105873. https://doi.org/10.1016/j.frl.2024.105873

76. Yuan, Y.C., Tu, Y., Zhang, G.R., & Cui, J.J. (2026). A Saliency-Fused Spatio-Temporal Graph Neural Network for Systemic Risk Early Warning in China's Financial-Real Economy. *IEEE ACCESS*, 14, 36573-36588. https://doi.org/10.1109/ACCESS.2026.3670479

77. Zhao, W.J., & Zhang, Z.L. (2022). A study on the dynamic distribution, spatial difference and convergence of regional financial risks in China’s eight comprehensive economic zones. *Operations Research and Management Science (in Chinese)*, 31 (3), 199-206. https://doi.org/10.1155/2022/9274737

78. Zhao, Y.L., Li, Y., Feng, C., Gong, C., & Tan, H.R. (2022). Early warning of systemic financial risk of local government implicit debt based on BP neural network model. *Systems*, 10 (6), 207.

79. Zhang, D.Y., Hu, M., & Ji, Q. (2020). Financial markets under the global pandemic of COVID-19. *Finance Research Letters*, 36, 101528. https://doi.org/10.1016/j.frl.2020.101528

80. Zhang, D., Wang, X., Qu, L., Li, S., Lin, Y., Yao, R., Zhou, X., & Li, J. (2020). Land use/cover predictions incorporating ecological security for the Yangtze River Delta region, China. *Ecological Indicators*, 119, 106841. https://doi.org/10.1016/j.ecolind.2020.106841

81. Zhang, L.G., & Teng, Z.J. (2021). Study on the spatial correlation and contagion mechanism of regional financial risks in China−empirical evidence based on social network analysis method and regional data. *Journal of Financial Development Research (in Chinese)*, (11), 48-55. https://doi.org/10.19647/j.cnki.37-1462/f.2021.11.007

82. Zhang, W., Zhuang, X., & Li, Y. (2019). Dynamic evolution process of financial impact path under the multidimensional spatial effect based on G20 financial network. *Physica A-Statistical Mechanics and its Applications,* 532, 121876. https://doi.org/10.1016/j.physa.2019.121876

83. Zhong, B., Liu, N., & Bi, S.R. (2002). Theory and practice of regional financial risk early warning system. *Journal of Financial Research (in Chinese)*, (7), 105-111.

84. Zhou, Z., Dong, K., & Wang, S.Y. (2012). An empirical study of financial contagion effect based on the European Sovereign debt crisis. *Management Review (in Chinese)*, 24 (2), 3-11. https://doi.org/10.14120/j.cnki.cn11-5057/f.2012.02.018

85. Zhuang, Y.Y., & Wei, H. (2023). Early warning model and prevention of regional financial risk integrated into legal system. *Plos One*, 18 (6), e0286685. https://doi.org/10.1371/JOURNAL.PONE.0286685

86. Zhou, J., Xie, C., Gong, S., Wen, Z., Zhao, X., Xuan, Q., & Yang, X. (2025). Data augmentation on Graphs: a technical survey. *ACM Computing Surveys.* https://doi.org/10.1145/3732282

87. Zou, Y.J., Chen, Q.H., Han, J.H., & Zhao, L.F. (2025). Analysis of the risk spillover network of G20 stock markets based on transfer entropy and complex network approaches. *Plos One*, 20 (12), e0336904. https://doi.org/10.1371/journal.pone.0336904

Contact information

Ph.D. Weiran Lin
Hangzhou City University
Department of Applied Statistics
China
E-mail: linwr@hzcu.edu.cn
ORCID: 0000-0002-4688-5225

https://doi.org/10.7441/joc.2026.03.01

Ph.D. Haijing Yu (Corresponding Author)
Xiangtan University
Business School
China
E-mail: yuhaijing1513875@163.com
ORCID: 0000-0002-6920-4517

Caihong Zhu
Hangzhou City University
Department of Applied Statistics
China
E-mail: 2250104001@stu.hzcu.edu.cn
ORCID: 0009-0002-4812-6721

https://doi.org/10.7441/joc.2026.03.01